



## Review

## Photoinduced electron transfer processes in fullerene–organic chromophore systems

Danuta Wróbel<sup>a,\*</sup>, Andrzej Graja<sup>b</sup><sup>a</sup> Faculty of Technical Physics, Institute of Physics, Poznan University of Technology, ul. Nieszawska 13A, 60-965 Poznań, Poland<sup>b</sup> Institute of Molecular Physics, Polish Academy of Sciences, ul. M. Smoluchowskiego 17, 60-179 Poznań, Poland

## Contents

1. Introduction.....	2556
2. Basic physical concepts of energy and electron transfer processes.....	2556
2.1. Excitation energy transfer – Förster and Dexter models.....	2556
2.2. Marcus theory of electron transfer.....	2556
2.3. Radiative and non-radiative quenching processes.....	2556
2.4. Photoinduced single- and multi-step electron transfer.....	2558
2.5. Ground state aggregates, excimers, exciplexes and charge-transfer complexes.....	2559
3. Fullerenes and monomolecular organic chromophores.....	2560
3.1. Physical properties and chemistry of fullerene.....	2560
3.2. Selected organic chromophores.....	2561
4. Studies of selected organic materials.....	2561
4.1. Donor–acceptor ensembles.....	2561
4.2. Fullerene–organic chromophore dyads, triads, tetrads.....	2565
4.3. Branched donor–acceptor ensembles and self-organised systems.....	2569
4.4. Molecular arrangement in Langmuir–Blodgett films.....	2572
5. Towards prospective applications.....	2574
Acknowledgements.....	2574
References.....	2575

## ARTICLE INFO

## Article history:

Received 8 September 2010

Accepted 23 December 2010

Available online 1 February 2011

## Keywords:

Electron/energy transfer

Organic chromophores

Fullerene

Donor–acceptor complexes

Langmuir–Blodgett films

Photovoltaics

## ABSTRACT

The review concentrates on supermolecular electron-donor–acceptor systems composed of porphyrin dyes covalently linked to fullerene. These model systems are of a great importance not only in optoelectronic technologies but also in the life sciences in relation to respiration, photosynthesis and photomedicine. Results of studies of supermolecular systems composed of zinc porphyrin and its dyad covalently linked to one fullerene or two fullerene molecules (in chloroform solution and in the form of Langmuir–Blodgett layers on a gold substrate) are presented to illustrate the spectroscopic properties and electron transfer processes taking place in such systems. Some simpler models of donor–acceptor ensembles are also presented. Electronic absorption and fluorescence supported by reflectance–absorption in infrared and electron spin resonance spectroscopies as well examination of light-induced current generated in photoelectrochemical cells were used to follow the interactions, radiative and non-radiative processes accompanied with electron transfer from an electron donating species to an electron acceptor. The same methods could provide information on modification of the electronic structure of the systems. The observed changes in absorption and fluorescence quenching of porphyrins in the presence of fullerene have evidently shown charge redistribution both upon porphyrins linkage to fullerene and upon deposition of the systems on gold substrate resulting from the interaction between the organic layers and the solid. The results reported in this paper prove the donor–acceptor character of the zinc porphyrin–fullerene samples and influence of fullerene on dye photoactivity in the systems.

© 2011 Elsevier B.V. All rights reserved.

\* Corresponding author. Tel.: +48 61 665 31 79; fax: +48 61 665 31 78.

E-mail address: [danuta.wrobel@put.poznan.pl](mailto:danuta.wrobel@put.poznan.pl) (D. Wróbel).

## 1. Introduction

One of the most important and interesting chemical reactions in nature is conversion of sunlight to chemical potential [1–7]. The physical cause of this effect is photoinduced electron transfer in the photosynthetic reaction centre. Recognition of the importance of these phenomena was emphasised by the Nobel Prize awarded to Marcus [8,9]. Photosynthesis has been widely investigated not only for understanding all aspects of this fascinating process but also because of its potential applications [10]. For instance, photoactive molecular devices and machines, which act as sensors, memories, and switches at a molecular level, have been extensively investigated aiming at replacement of conventional electronic devices by molecular systems.

Intermolecular photoinduced energy and electron transfers are simple processes in which the energy of an electron is transferred from a donating species to an accepting species, producing the radical cation of the donor and the radical anion of the acceptor, when one of these species is photoexcited [11–13]. An obvious approach to achieve efficient and rapid electron transfer is covalently linked donor and acceptor moieties, and indeed many types of such donor–spacer–acceptor molecular systems have been synthesized and studied [5–7,10,11,14,15]. Construction of efficient artificial photoactive devices is based on the following requirements: (1) the light must be captured by antenna molecules leading to excited states, (2) the absorption of light must result in transfer of an electron to the acceptor, (3) the electron transfer must be directional, and (4) the lifetimes of the excited states must be long enough for electron transfer to take place [11]. Porphyrins used as dyes and covalently linked quinines as electron acceptors have been for a long time used as systems imitating photosynthetic reaction centres [14]. Recently, there has been a great deal of interest in fullerene  $C_{60}$  as an ultimate electron acceptor in multi-step intramolecular photoinduced electron transfer reactions [15]. Fullerenes exhibit a number of characteristic electronic and photophysical properties, which make them promising candidates for investigation of photoinduced electron transfer [15–19]. For this reason fullerenes are now commonly used for electron-transfer studies and construction of molecular electronic devices.

In this article recent developments in the area of the photoinduced electron transfer in molecular systems type fullerene–organic chromophore are presented. The physical basis of photoinduced electron transfer as well as typical photoactive materials and the commonly used methods of their investigation are also summarised.

## 2. Basic physical concepts of energy and electron transfer processes

### 2.1. Excitation energy transfer – Förster and Dexter models

Energy and electron transfers are central processes in physics, chemistry and biology and they play essential role in all branches of life sciences and technology; e.g. in photosynthesis [20], vision [21], respiration [22], catalysis [23], photomedicine [24] and in optoelectronics in informative storage devices and photoelectric devices like for example photovoltaic cells and light emitting diodes [25,26] and everywhere where the absorbed photon drives charge separation and energy/electron transfer.

There are certain phenomena and processes essential for effectiveness of the solar energy use in optoelectronic devices based on molecular systems. They include strong  $\pi$ – $\pi$  absorption (absorption coefficient must be  $>10^5 \text{ cm}^{-1}$ ), very fast electron donor–acceptor transfer followed by charge separation, slow charge recombination, efficient energy transfer between a donor

and an acceptor. Also very important is the molecular system arrangement since molecular organisation determines markedly the excitation energy/electron transport [27].

In this chapter we will focus on the energy and electron transfer mechanisms which govern processes occurring after radiative absorption. Let's start with basic theoretical background. The first concept on the excitation energy transfer came from Förster in 1948/1949 [28] and his idea has been developed over the past few decades [29–34]. Förster long-range resonance excitation energy transfer (FRET) [35] is potentially very sensitive to proximities in the nanoscale range, i.e. to the distance between donor and acceptor. According to the Förster theory when the Coulomb interaction between donor (D) and acceptor (A) the dipole moment interaction can be approximated by the dipole–dipole term. In the strong coupling interaction (when energy of interaction between D and A is greater than the width of the transitions) the energy transfer process is classified by Dexter to occur according to the exchange mechanism [36], which requires overlapping of wave functions of D and A. The excitation is delocalized over D and A and oscillates back and forth between them. The schemes of FRET and Dexter models are presented in Fig. 2.1.

The energy transfer process described by the Förster model takes place when the distances between D and A range from about 5 Å to about 100 Å. When the separation in the D–A pair is much closer ( $R \leq 5 \text{ Å}$ ) the energy transfer process is described as according to the Dexter mechanism. The fluorescence lifetime of D is of the order of  $10^{-8}$ – $10^{-9}$  s. The energy transfer rate constants can range from  $10^9$  to  $10^{14} \text{ s}^{-1}$  depending strongly on the type of system and mechanisms responsible for the processes.

### 2.2. Marcus theory of electron transfer

The electron transfer theory was originally proposed by Marcus in 1956 [37] and has been developed through the past few decades [38–40] to explain outer electron transfer (ET) from the electron donor to the electron acceptor in the system in which two chemical species are not directly bonded to each other. The Marcus theory was extended to the inner sphere ET model [41] in which two chemical species are linked by a chemical bridge. Marcus theory has been also extended to address heterogeneous electron transfer. In heterogeneous ET an electron moves between a chemical species and a solid-state electrode. The last models addressing heterogeneous electron transfer can find applications in electrochemistry and in solar cell design. Various modifications of the Marcus theory have been proposed in bioenergetics and in technology, e.g. photochemical proton transfer model including incorporation of asymmetry [42], enzymatic proton transfer [43], description of organometallic reactions [44], corrosion, catalysis or any kind of redox processes [45–49].

The simple model of ET can be presented as  $D + A \rightarrow D^+ + A^-$ . In the energetic diagram of free energy versus reaction coordinate (Fig. 2.2) the key parameters  $J$ ,  $\Delta G^\circ$  and  $\lambda$  are presented.

The left and right hand parabolas represent the potential energy surface of the nuclear motion of the compounds in the initial (the electron is still on the D species) and in the final state (the electron has been transferred from D to A), respectively. The energy reorganisation  $\lambda$  is a sum of internal energy  $\lambda_i$  (connected with changes in molecular geometry at the transition from the neutral molecule to its ion) and energy of outer reorganisation,  $\lambda_o$ , which is related to solvent rearrangement coordinating the charged molecules of products.

### 2.3. Radiative and non-radiative quenching processes

A molecule when excited to higher energetic state comes back to its ground state (if it does not chemically react with other

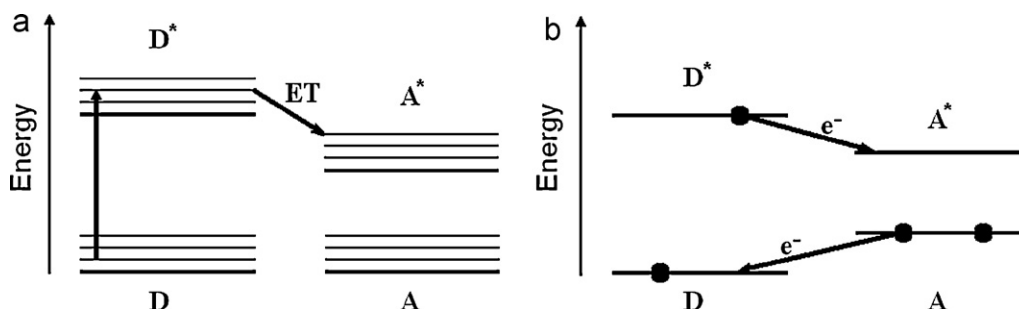


Fig. 2.1. Scheme of Förster and Dexter models; A – acceptor, A\* – excited acceptor, D – donor, D\* – excited donor, ET – energy transfer.

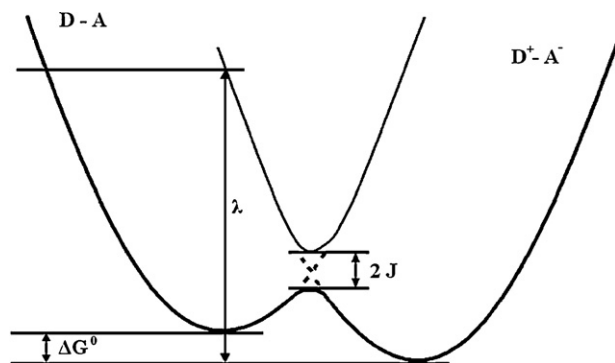


Fig. 2.2. Energy diagram of the initial and final stage of reactant and product:  $J$  – electronic coupling between the initial and final states,  $\Delta G^0$  – total Gibbs free energy,  $\lambda$  – reorganization energy.

molecules) and its excitation energy is dissipated in deactivation processes. In the molecules, the excess of energy can be deactivated by radiative and non-radiative intramolecular (one-molecular) processes or can be absorbed in external and intermolecular interactions (bi- and multi-molecular) [50]. All these processes have to occur in a time shorter than the natural lifetime of the excited state of the molecules. The excess energy can be emitted from the molecule as fluorescence, phosphorescence or delayed luminescence or changed into thermal energy. In the presence of a molecular neighbour, the energy can be transferred to another molecule, or used for charge separation and electron transfer process to other molecules (Fig. 2.3). The sum of yields of these processes in accordance with the energy conservation law can be expressed as a sum of quantum yields of emission ( $\Phi_E$ ), energy/electron transfer ( $\Phi_{ET}$ ), thermal deactivation ( $\Phi_{TD}$ ), charge separation ( $\Phi_{CS}$ ), and other processes of deactivation.

There is a close competition among deactivation processes both radiative and non-radiative. Schemes of some processes occurring in a system composed of energy/electron donor and acceptor systems are shown in the Jabłoński diagram presented in Fig. 2.4. For example the fluorescence process can compete with charge separation and electron transfer and can lead to decrease in the photovoltaic effect effectiveness.

As we have done in our study, the  $\pi$ -electronic singlet state features can be studied by the absorption and fluorescence spectroscopies [51]. Electron transfer processes in the donor–acceptor systems can be investigated by, e.g. fluorescence quenching [52] and electron spin resonance (ESR) [53,54]. Behaviour of the triplet states can be also studied by phosphorescence examination as well as by the use of laser-induced photothermal spectroscopy (LIOAS) introduced by Braslavsky [55,56], supported by photoacoustic spectroscopy (PAS) proposed by Rosenzweig [57]. PAS is a nondestructive spectroscopic tool which uses light and sound to probe materials and follow processes like, e.g. non-transparent samples, inhomogeneous materials, surfaces, bulk materials, thin films [57] as well heat transport in complex structures, fluorescence quantum yields in scattering samples [58], energy transfer yields rates in chemically stable materials [59] as well chemical reactions and others [60]. Time-resolved photoacoustic calorimetry can be used to measure the energy released upon injection of an electron from an electronically excited dye adsorbed to nanocrystalline  $\text{TiO}_2$  into the conduction band [61]. In slow thermal deactivations (in the range of microseconds) triplet states are usually involved whereas the singlet states contribute to fast deactivations. The main components in the PAS device are a photoacoustic chamber filled with proper gas and with a sample (the latter one is excited with the modulated light beam) and a very sensitive microphone (converting thermal signal coming from a sample to an acoustic one) [55]. With a good experimental setup (the proper optical and thermal lengths, thickness of a sample) [57] the photoacoustic sig-

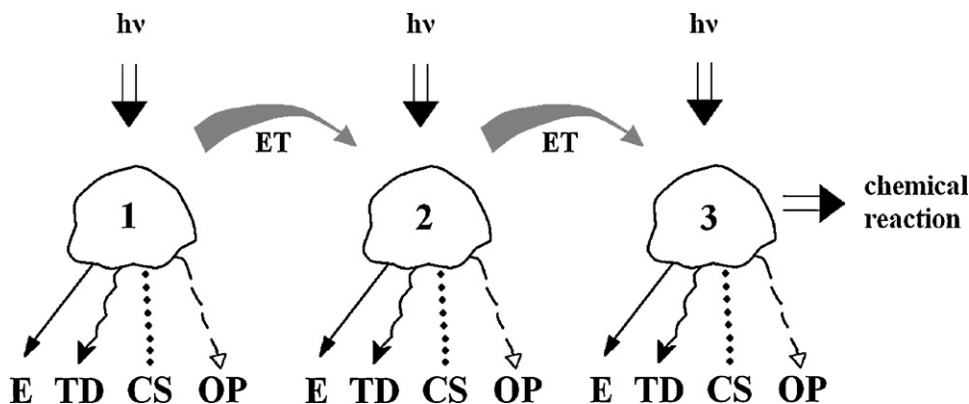
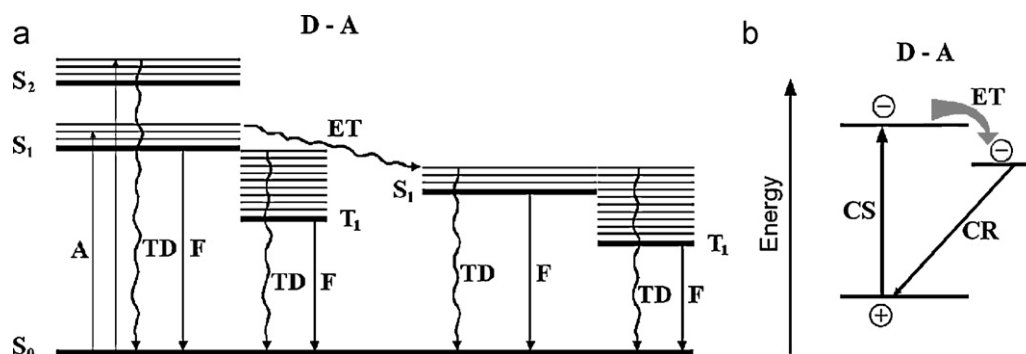


Fig. 2.3. Scheme of energy pathways in a donor–acceptor chain in molecular system of 1–3 components:  $h\nu$  – quantum of energy, E – emission, ET – energy and/or electron transfer, TD – thermal deactivation, CS – charge separation, OP – other processes.



**Fig. 2.4.** Scheme of some radiative (straight line) and non-radiative processes (wave line) in the energy donor–acceptor (D–A) system –  $S_0$ ,  $S_1$ ,  $S_2$  – singlet ground and excited states,  $T_1$  – triplet state, ET – energy transfer, F – fluorescence, TD – thermal deactivation (a) and model of charge separation (CS), electron transfer (ET), charge recombination (CR) in D–A system (b).

nal depends on optical and thermal properties of materials. The PAS experiment provides global information on thermal transitions originating from various species in the studied materials. The thermal deactivation parameters can be expressed as a rate of an absorbance and a photoacoustic signal. These parameters describe thermal properties of the samples. With the use of different light modulation frequencies, it is possible to evaluate the contribution of slow signals (micro- to millisecond) originated from metastable states and that contribute very promptly (in femto-, pico-, nanosecond) as proposed in [62,63] and used successfully in our laboratory. To distinguish the fast thermal deactivation processes from the slow transitions the LIOAS examinations can be applied. This technique allows one to distinguish fast thermal transitions from those of microsecond time duration (usually, the experimental resolution of a signal is 0.3–0.8  $\mu$ s) and evaluate population of triplet states as well as their thermal relaxation. A nitrogen laser (337.1 nm) and a dye laser are used as light sources. A thermoelastic effect caused by periodic irradiation of the sample gives mechanical oscillations and thermal signal is detected by a piezodetector [55]. The PAS and LIOAS spectroscopies are successfully used in our laboratory in investigation photoactive organic materials suitable for photovoltaics, photodynamic therapy or in modelling photosynthesis [e.g. 64–67]. Bimolecular interactions could also yield delayed luminescence (DL) and the DL experiment have been used to study the charge recombination in some porphyrin systems [68]. These methods have been used in our investigations presented in this paper and the results have contributed to our knowledge of the electronic states of the molecular systems and of the interactions between donor and acceptor species in the systems under investigation.

#### 2.4. Photoinduced single- and multi-step electron transfer

As mentioned above, fast photo-induced electron separation (CS) and charge recombination (CR) processes are essential in optoelectronics. Photoinduced single-step electron transfer can be discussed in the conventional D–A pair or covalently linked dyad (or higher molecular architecture) as the simple model pro-

cess. Typical examples could be, e.g. porphyrin–quinone mixtures, porphyrin–porphyrin dyads or photovoltaic systems with chromophores interacting with an electrode. The single-step electron transfer that involves D–A pairs can be schematically be described as  $D-A + h\nu \rightarrow D^* - A \rightarrow D^{\bullet+} - A^{\bullet-}$  (Fig. 2.5a).

In the single-step electron transfer process molecules D play a double function, they act as antenna molecules that harvest excitation and as a primary electron donors that transfer an electron to an acceptor. The photoexcitation of a donor and in sequence of an acceptor leads to formation of a pair of donor (radical cation) and acceptor (anionic radical) which recombine rapidly to the initial state of the system [69]. The multi-step electron transfer is crucial in, e.g. photosynthesis, photocatalysis, and any process in which charge separations with a cascade of photoinduced electron transfers in the D–A systems take place. In the multi-step electron transfer at least three species have to be involved: donor–acceptor(1)–acceptor(2),  $D-A^{(1)}-A^{(2)}$ , in which  $A^{(1)}$  and  $A^{(2)}$  are primary and secondary acceptors, respectively [5,70,71]. In each stage of electron transfer chain the gradient of energy is required in accordance with the sequence:  $D-A^{(1)}-A^{(2)} + h\nu \rightarrow D^* - A^{(1)} - A^{(2)} \rightarrow D^{\bullet+} - A^{(1)\bullet-} - A^{(2)} \rightarrow D^{\bullet+} - A^{(1)} - A^{(2)\bullet-}$  [70,71]. The scheme of these processes is shown in Fig. 2.5b. The electron transfer between the first acceptor  $A^{(1)}$  and the second one  $A^{(2)}$  competes with the processes of energy dissipation, e.g. in the CR, IC and ISC processes, leading to the initial state of the system. Also fluorescence is strongly quenched when electron transfer occurs in a system (the quantum model of fluorescence quenching by electron transfer is shown in Fig. 2.6).

The distance between molecules D and A, suitable redox potentials and excitation energy play essential roles in the optimisation of the electron transfer rate. The lifetime of the charge separated state in the  $D-A^{(1)}-A^{(2)}$  system (Fig. 2.5b) is longer than that in the single-step D–A one (Fig. 2.5a) because the distances between molecules in  $D-A^{(1)}-A^{(2)}$  are greater than that between molecules in the D–A systems. According to the Marcus theory, reorganisation energy is a vital criterion in optimising effectiveness of fast CS and in diminishing CR; low reorganisation energy is required for the

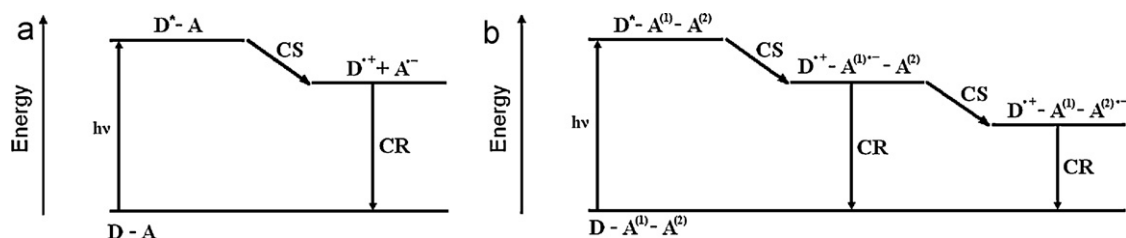


**Fig. 2.5.** Quantum models of single-step (a) and multi-step (b) electron transfer.



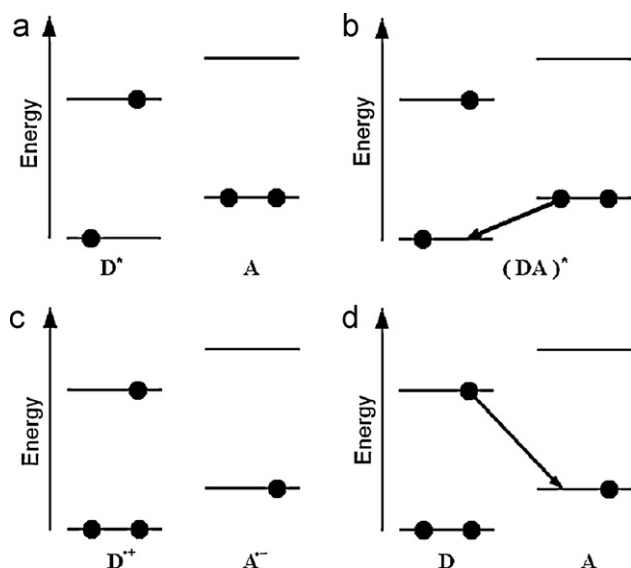


**Fig. 2.6.** Scheme of donor (D) fluorescence quenching by electron transfer to acceptor (A) –  $D^*$  – excited donor,  $D^{\bullet+}$  – donor radical,  $A^{\bullet-}$  – acceptor radical; (a–d) – stages of electron transfer.

fast CS and slow CR processes [5]. For this reason, the fullerenes are families of molecular species characterised by low reorganisation energy, strong electronic coupling,  $\pi$ -electron delocalization and rigid structure which make them perfect molecular systems of excellent electron acceptor properties [72,73].

Intermolecular single-step and multi-step electron transfer processes in the D–A systems have been systematically studied by Gust et al. [73], Imahori et al. [5,6,72,74], Sariciftci [75], Moore et al. [76], Tkachenko et al. [77], Guldi et al. [78], Kato et al. [79], Hudhomme et al. [80], Bonifazi et al. [17] and many others. There are a number of papers devoted to investigation of photophysical processes occurring in D–A systems, dynamics of charge separation, electron transfer and charge recombination as well applications of these models in nanostructured artificial photosynthesis and molecular photodevices [5,6,17,69–84]. Single-step electron transfer realised by ultra-fast charge shift was reported for the strongly coupled zinc porphyrin–gold porphyrin dyads, whose lifetime is in the order of hundreds of picoseconds [81]. Also the conventional single-step electron transfer models like, e.g. porphyrin with quinone [70] and porphyrin–diimide [82] have been presented. Many other papers have been devoted to more complicated systems like triads or higher adducts containing porphyrin or other chromophores and different fullerenes (e.g.  $C_{60}$ ,  $C_{70}$ ,  $C_{76}$ ,  $C_{78}$ ) with multi-step electron transfer and long-range charge separations [5,6,17,70–80,83,84]. In chromophore–fullerene dyads and more complicated triads or pentads the CS state lifetime can be extended even up to 120 s [6] and the ratios of CS rate to CR rate are much higher than those in conventional D–A species [5,6], therefore their photovoltaic effects are expected to be much more effective.

## 2.5. Ground state aggregates, excimers, exciplexes and charge-transfer complexes

Molecular aggregates play important roles in many areas of physics and chemistry, in molecular crystals [85,86], non-crystalline molecular systems with van der Waals and hydrogen interactions [87], covalently bonded supermolecular units [88], in modelling of the structure of photosynthetic organisms and processes [89], modern optoelectronics [25] and in production of organic semiconductors [87,90]. Molecular aggregates can reduce photoactivity of systems. A very important aspect that needs to be

considered is a strong tendency of chromophore molecules to form aggregates and other structures as a result of mutual interactions. These effects are important in potential applications of molecular systems in optoelectronics.

The formation of aggregated structures and their spectroscopic properties have been studied by Kautsky et al. [91], Levison et al. [92] and Szent-Györgyi [93] but described theoretically by Förster in his quasi-classic vector model [94] and in the exciton model proposed by Kasha [86].

Changes in photophysical features of the aggregates can be easily detected by absorption and fluorescence investigations. Their modifications depend on the type of aggregates and are manifested by the appearance of strong band shifts (of up to about  $2000\text{ cm}^{-1}$ ) or by splitting of the absorption bands as well changes in the band widths [95]. Also, the fluorescence quenching and changes in thermal deactivation could be associated with aggregate formation due to the enhancement of triplet state population [96,97]. The aggregate structures differ from one another by geometrical arrangement of their dipole moments: in the ideal H aggregates, the molecular frames are oriented face-to-face with parallel transition dipole moments of interacting monomer units oriented perpendicularly to the line joining the molecular centres. Otherwise, in the ideal J aggregates the polarisation axis for the in-line transition dipoles is directed along the line joining the molecular centres. In double molecules with the coplanar transition dipoles inclined to the axis connecting the molecules' centres, the angle between the dipole moment's directions varies from  $54.7^\circ$  to  $90^\circ$  and  $0$  to  $54.7^\circ$  in H and J, respectively [98–101]. The blue and red absorption shifts ( $1000$ – $2500\text{ cm}^{-1}$ ) are expected to appear in the absorption spectra of the H and J aggregates, respectively, and they correspond to increasing and lowering energy [2,102]. The H dimers have been extensively studied in a number of papers and they show characteristic fluorescence quenching [103,104]. The formation of fluorescent J-dimers has been the subject of some studies [105]. According to the Kasha vector model [86] the existence of the oblique transition dipoles of aggregated species is also possible. In the oblique transition configuration, the dipole transitions polarised mutually perpendicularly and the configuration of the dipole arrangement (as a composition of in-phase transition dipole arrangement and out-of-phase one) leads to the decreased energy and increased energy of the excited states of dimerized molecules. Also, considerable changes can be observed in their fluorescence behaviour and thus in consequence of non-radiative processes; thermal relaxation is expected to be changed in aggregated dyes [106]. The results of the exciton model study, presented in [86], show that in aromatic aggregates a triplet state population increases due to the interaction of the component molecules. In some cases fluorescence competes with another phenomenon leading to decreased fluorescence, shortening of its lifetime and increased triplet population [107]. However, for weakly interacting molecule species no significant changes in absorption and in fluorescence are observed. Nevertheless, it is possible to follow weakly interacting molecules by complementary spectroscopic methods – PAS and LIOAS [108–110].

Excimers (excited state dimers) and exciplexes (excited complexes) [111] are short-lived dimeric or heterodimeric molecules formed from two species one of which is in the electronic excited state. Excimers/exciplexes are often bimolecular species that would not be bonded if both were in the ground state. The lifetime of excimers is of the order of nanoseconds. The formation of an excimer is promoted by high monomer packing and can be studied by fluorescence spectroscopy; its emission wavelength is longer than that of the excited monomers because of its lower energy level. Fig. 2.7a, c and d present the quantum model of an excimer and its emission features. There are some literature data on the use of excimers in laser technology [112], intra- and intermolecular

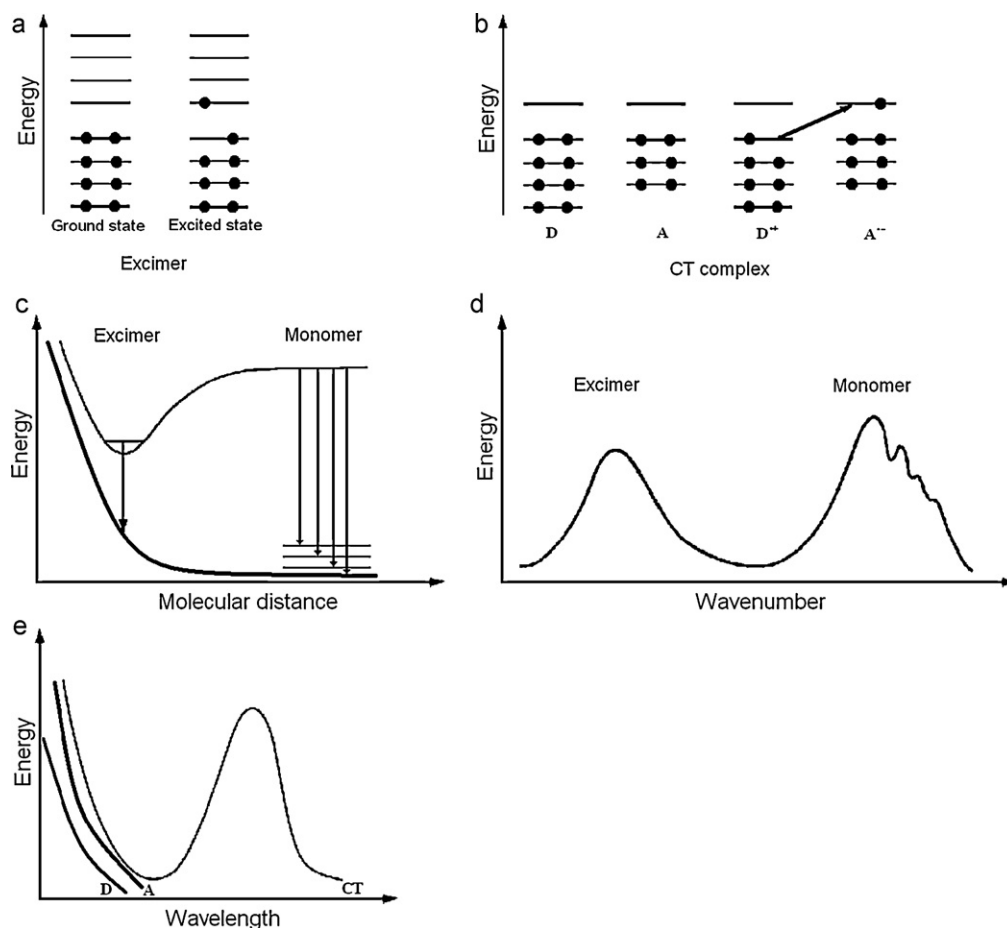


Fig. 2.7. Quantum models of excimer (a), CT complex (b), excimer energy curves (c), excimer fluorescence spectrum (d), CT absorption spectrum (e).

interactions [113], singlet-singlet energy migration study [114], as sensitive probes of ribonucleic acid sequence and structure [115] as well as in examinations of conformation changes [116]. In the supermolecular systems like, *e.g.* porphyrin–fullerene species, the excimer formation was also observed [117], which confirms strong interaction between chromophore and C<sub>60</sub> in the covalent complex. A charge-transfer complex (CT complex) or D–A complex are chemical associations of two or more molecules, or of different parts of one very large molecule, in which the attraction between molecules (or parts) is induced by an electronic transition into an excited electronic state. In such systems a fraction of electronic charge is transferred between the molecular entities. The resulting electrostatic attraction provides a stabilizing force for the molecular complex.

Charge-transfer complexes exist in many types of molecules, both inorganic and organic. Optical spectroscopy, particularly absorption and resonance Raman techniques are powerful methods to characterise CT. The quantum model of CT complex and its absorption is shown in Fig. 2.7b and e. In CT complexes, characteristic changes in colours take place as a result of charge-transfer transition energy, which is typical of specific type of donor and acceptor entities. The absorption bands of CT complexes are well recognised. Their colour reflects the relative energy balance resulting from the transfer of electronic charge from an electron donor to an electron acceptor and varies with changes in solvent permittivity. The CT complexes play an essential function in many branches of physics, chemistry and biology [118]. A perfect example of strong CT complex is tetracyano-*p*-quinodimethane (TCNQ) as a strong acceptor and tetrathiafulvalene (TTF) as a good donor; this complex

shows one-dimensional electrical conductivity in a stacked crystalline solid [119]. Another nice example is CT of lycopene-iodine associate, which can find application in bio-solid state solar cells [120]. A strong charge-transfer band in the UV region in a solution of Ag<sup>+</sup> ions and deoxyribonucleic acid-wrapped carbon nanotubes has been also observed [121].

### 3. Fullerenes and monomolecular organic chromophores

#### 3.1. Physical properties and chemistry of fullerene

The unique chemical and physical properties of fullerene C<sub>60</sub> such as its highly efficient electron acceptor character and electronic absorption throughout the UV–vis spectral region, have aroused considerable interest in its role in covalent donor–acceptor systems [5,18,19,122–125]. The special properties of fullerenes are directly related to the very high symmetry of the C<sub>60</sub> molecule (point group I<sub>h</sub>), in which 60 equivalent carbon atoms are at the vertices of a regular truncated icosahedron; each carbon site on C<sub>60</sub> is trigonally bonded to other carbon atoms.

Group theory indicates that 10 of the 46 vibrational mode frequencies are Raman-active, 4 are IR-active and the remaining 32 are optically silent. The fullerene C<sub>60</sub> absorbs strongly in the UV range ( $\epsilon_{\text{max}} \sim 10^5 \text{ M}^{-1} \text{ cm}^{-1}$ ) and much more weakly in the visible region ( $\epsilon_{\text{max}} \sim 710 \text{ M}^{-1} \text{ cm}^{-1}$ ) for the symmetry reasons [126]. The visible absorption is allowed only because of vibronic interactions and it is observed at about 455 nm. The main UV absorption bands of C<sub>60</sub> in cyclohexane solution are at 266 and 343 nm (Fig. 3.1).

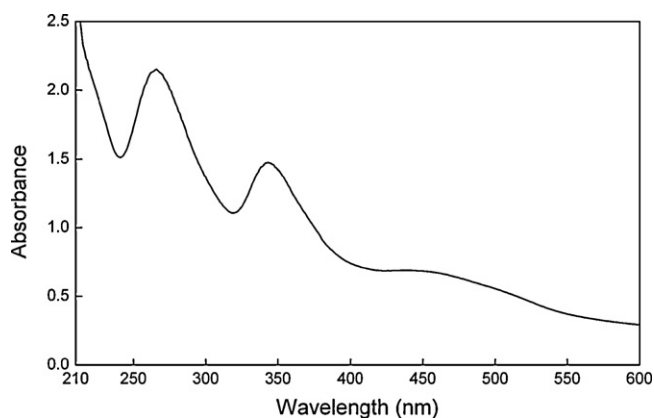


Fig. 3.1. Electronic absorption spectrum of  $C_{60}$  in cyclohexane.

A very low emission quantum yield ( $10^{-4}$ ), associated with the singlet excited state, is a result of a combination of a short lifetime, a quantitative intersystem crossing and, finally, the symmetry forbidden nature of the lowest-energy transition. To the some extent, the phosphorescence quantum yield ( $10^{-6}$ ) is strongly impacted by the spherical structure of  $C_{60}$  [16,18,127]. Analysis of fluorescence spectra of the fullerene in organic solvents indicates that the intensity of fluorescence bands and their fine structure are strongly dependent on the interaction between  $C_{60}$  and the solvent.

For construction of optoelectronic devices or artificial photosynthetic systems the charge separation originating from photoinduced electron-transfer is of utmost importance [5]. To optimise this process the contact between the fullerene (electron-accepting molecule) and electron-donating molecule (e.g. organic dye) must be very close. The best way to optimise the contact between both moieties of the system is to induce covalent bonding of the parts [2,7,19]. All reactions of  $C_{60}$  take place at the double bond between the 6-membered rings (pyracylene unit) (Fig. 3.2) to give dihydrofullerenes as the initial product [128]. Simple and high-yield route to dihydrofullerenes is Diels–Alder addition of electron-rich dienes to  $C_{60}$  [129]. This is a very versatile route which allows easy variation of functional groups and considerable control of the solubility of the adducts [130].

### 3.2. Selected organic chromophores

Porphyrins are composed of four pyrrolic macrocycles connected via methine bridges. Differences in the spectra of substituted porphyrins and other related macrocycles come from perturbations in energy states due to the presence of metal, substituents or peripheries of conjugated ring systems, the number and type of ligands, solvent conditions and degree of aggregation and its architecture, which can occur via direct or indirect interaction [88,131–133]. In phthalocyanines, similar to porphyrins, four indole units are conjugated with nitrogen bridges. Porphyrins are characterised by strong absorption bands at about 420–450 nm (Soret region) with high molar absorption coefficient of the order of  $10^5 \text{ M}^{-1} \text{ cm}^{-1}$  and much less intense Q bands in the long wavelength region 500–650 nm [134]. In the spectra of phthalocyanines the Q bands in the long-wavelength region (650–680 nm) are strong, while less intense bands appear in the range of the Soret bands [135]. Most of the porphyrin dyes show intensive fluorescence in the range 600–800 nm. The fluorescence lifetime values of many of porphyrins and phthalocyanines range from about 1 to 15 ns with the corresponding fluorescence quantum yields of 1 to nearly 15%.

Polycyclic aromatic hydrocarbons are chemical compounds that consist of fused aromatic rings and do not contain heteroatoms

or carry any substituents. One of the most interesting representatives of this group is perylene of the chemical formula  $C_{20}H_{12}$ . Perylene shows maximum absorption at 434 nm with the molar absorption coefficient of  $38\,500 \text{ M}^{-1} \text{ cm}^{-1}$ . Pure or substituted perylenes exhibit high fluorescence quantum yields [136,137] and high photo- and thermal stability as well as chemical inertness [138].

Perylene diimides (PDI) are well-known as chemically and thermally stable light-harvesting dye. Electronic structure of PDI is highly affected by introducing electron-donating or electron-withdrawing groups at the perylene core [139], which permits modification of the PDI photophysical properties. High photo- and thermal stabilities in the visible region and fluorescence quantum yields near unity ( $\Phi_F \approx 1$ ) make PDI suitable standards in fluorescence ( $\lambda_{em} \approx 500\text{--}600 \text{ nm}$ ) quantum yield measurements [138,140]. The electronic absorption spectrum of PDI in KBr pellet is dominated by typical perylene triple absorption with local maxima at 527, 493, and 458 nm; the spectrum also shows weak bands at 429, 277, and 224 nm [141].

Another interesting group of dyes are aromatic heterocyclic compounds. A representative of this group is thiophene of the formula  $C_4H_4S$ , consisting of a flat five-membered ring. Thiophenes are important compounds used as building blocks in many chemical syntheses [142]. Moreover, thiophene oligomers and thiophene-based molecules show interesting properties such as ready accessibility, easy structural modifications, high  $\pi$ -conjugation, low oxidation potential and environmental stability [143,144].

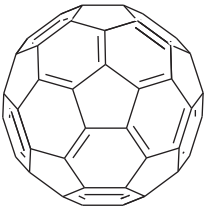
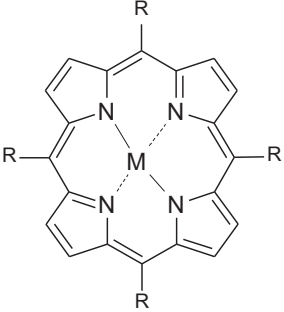
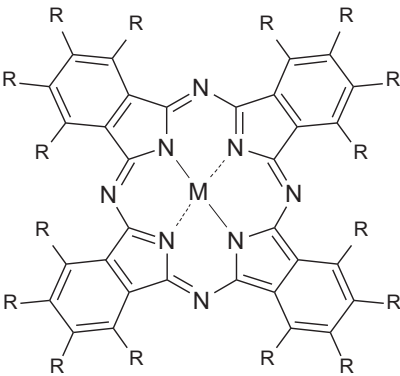
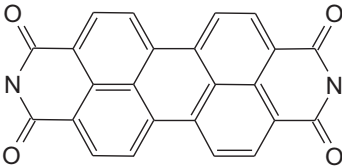
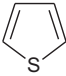
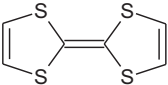
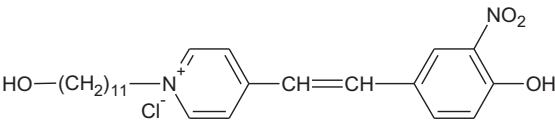
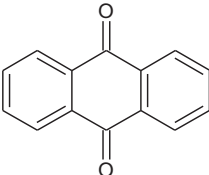
## 4. Studies of selected organic materials

### 4.1. Donor–acceptor ensembles

Studies of solar-light energy conversion based on the use of organic substances began by O'Regan and Grätzel [145] in 1991, have opened a new era in engineering of materials suitable for organic photovoltaics as renewable device in electricity generation. Since the end of the 20th century extensive development of new molecular materials acting as photoactive sensitisers and profound progress in design, construction and production of new photovoltaic devices have been observed. In the first dye-sensitised photovoltaics (DSPV), the photoactive molecules were sensitive to the UV and blue light [146–149], however over the past few decades intense research to improve DSPV has brought a great evolution in photocell design that stemmed from the use of a series of ruthenium–pyridine complexes working in DSPV as photosensitisers [147–149]. The first successful solid-hybrid dye-sensitised solar cells were reported to improve electron transport [150]. In [151] the authors reported the organic cell of efficiencies of 8.2% obtained with the use of solvent-free liquid redox electrolyte of a melt of three salts, as an alternative to using organic solvents as an electrolyte solution with efficiency of 11%. Numerous research groups have experimented with a wide variety of organic dyes based on porphyrins or phthalocyanines and DSPV with these materials reached the efficiency of the order of about 5–6% [151,152].

We present three simple models, in which the occurrence of electron and energy transfer processes, initiated by absorbed photon, is proved with the use of conventional spectroscopic methods. The first model, which is a photoelectrochemical cell (PEC) sensitised by porphyrin or phthalocyanine dyes is based on a correlation between the molecular structure of dyes and their ability to generate photocurrent followed by absorption spectroscopy and photovoltaic responses [66,153–163]. In the experiments, selected groups of the  $\pi$ -electron conjugated dyes have been used whose molecular structures are collected in Table 1.

**Table 1**  
Molecular structure of main donors and acceptors used.

Molecular structure	Chemical name	Abbreviated name
	Fullerene	C <sub>60</sub>
	Porphyrin (where M = H <sub>2</sub> , Mg, Zn, Cu, Pb and R = phenyl, naphthyl)	P
	Phthalocyanine (where M = Zn, Cu and R = TNP, F <sub>16</sub> , Cl <sub>16</sub> , (C <sub>n</sub> H <sub>2n+1</sub> ) <sub>8</sub> )	Pc
	Perylene-3,4,9,10-tetracarboxydiimides	PDI
	Thiophene	T
	Tetrathiafulvalene	TTF
	Stilbene merocyanine	SM
	Anthraquinone	AQ



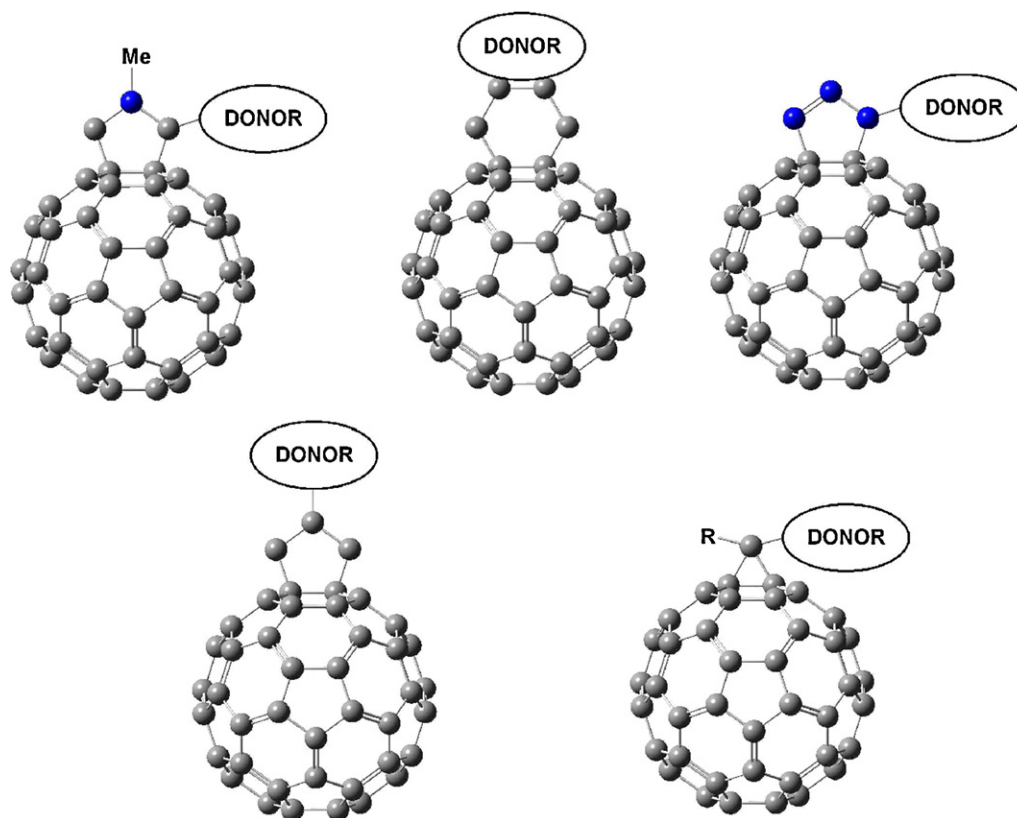


Fig. 3.2. Strategies to build up dye–fullerene assemblies using the [4 + 2] Diels–Alder cycloaddition of  $C_{60}$ .

Photovoltaic action spectra (photovoltaic response as a function of excitation wavelength), kinetics of photocurrent generation (in the second time scale) and current–voltage characteristics studies have been supported by spectroscopic investigations (absorption, fluorescence, photoacoustic and ESR spectroscopies). Coincidence of absorption and photovoltaic spectra evidently indicates the dyes responsibility for photovoltaic responses [69]. It is well known from literature that  $\pi$ -electron system is responsible for photovoltaic effects [69,135,159], however metal is able to change distribution of the  $\pi$ -electron cloud since the HOMO–LUMO transitions are influenced by the central atom [134]. Comparison of the photocurrent signals induced by light in PEC filled with metallic and non-metallic dyes shows evidently a strong influence of the type of metal ion built at the porphyrin or porphyrazine centres on the intensity of generated photocurrent signals [164,165]. Exemplary results of photocurrent generation are presented in Fig. 4.1. The dyes with Zn and Mg give the highest photocurrent [161,164], whereas their counterparts complexed with lead (Pb) showed very weak or even no photovoltaic response [161,165,166]. This result seems to be very interesting in view of chlorophyll and some bacteriochlorophyll pigments with magnesium and zinc ions in central rings, respectively [20,167]. Also the presence of the extra aromatic rings attached to the porphyrin or indole units in macro rings usually enhanced photoresponses of the dyes due to higher number of  $\pi$ -electrons and their delocalization [165,168]. However, the decline of the photosignals is observed when the long alkyl or alkyloxy chains are attached since most of the energy absorbed is lost in non-radiative processes [166]. The most interesting results are found with halogenated phthalocyanines. For PEC with fluorine or chlorine phthalocyanines ( $ZnPcF_{16}$ ,  $ZnPcCl_{12}$ ) fluorine and chlorine atoms attached externally to the main molecular macro ring strongly perturb the electron density distribution

because of the resonance coupling with the  $\pi$ -electron systems [66,162,163,168–170].

In the last decade various types of photovoltaic devices containing porphyrins, phthalocyanines and other chromophores of different structures and bonded with different peripheral substituents or groups were characterised and their activity as photosensitiser in photocurrent generation were studied by numerous

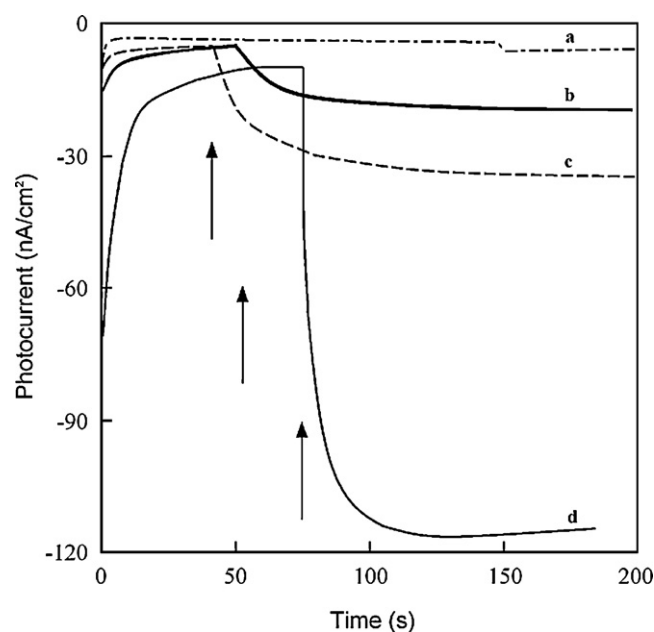


Fig. 4.1. Photocurrent signals of  $H_2TPP$  (a),  $ZnPcAlkyl$  (b),  $ZnPc$  (c),  $ZnPcF_{16}$  (d). The arrows indicate light on.

authors [171–179]. Many new dye-sensitised solar cells based on porphyrins have been tested with the use of, e.g. functionalised terthiophene building blocks [171–173]. For examples porphyrins and related macrocycles (tetraphenyl-, tetrabutyl-, tetramethyl- and tetrapyrldylporphyrins) and porphyrin having rhodamine moieties or other systems like porphyrin and ruthenium complexes have been also extensively reported as photosensitisers for developing photoelectrochemical solar cells [171,172,177–179]. Also porphyrin-sensitized  $\text{TiO}_2$  or a system with porphyrin–gold nanoparticles [174–176] were demonstrated as materials for a new cell that converts light energy into electricity. The studies present the results of the chromophore-based DSPV devices with different working media: from traditional organic liquid electrolytes, ionic liquid electrolytes, polymer gel electrolytes, quasi-solid state to self-assembled monolayer Schottky barrier cells, and other systems [171–179]. In many cases these DSPV systems offer high photovoltaic effects, chemical and thermal stability as well as opportunity for developing long-term operational solar cells and show how important is to give insight into knowledge on system constructions and on correlation between the molecular structure of dyes and their ability to photocurrent generation [66,69,161–179].

The second model of PEC assumes the presence of a mixture of dyes that absorb at different wavelengths of the solar spectrum. An interesting problem is the effect of energy transfer processes between photoactive dye species on the performance of photovoltaic devices. Two groups of dyes were selected: MgTNP and ZnPC (good photoconverters in photocurrent generation) and stilbene merocyanine (SM) (poor photoconverter in photocurrent generation, but thermally very efficient). The SM dye fills the solar energy gap in a wide range (Fig. 4.2a and b) [180]. As follows from the absorption, fluorescence and photoacoustic experiments, the intermolecular energy transfer between SM and MgTNP is efficient. When both dyes SM and MgTNP are embedded as a mixture in PEC, a marked enhancement of photocurrent intensity is observed, mostly due to effective energy transfer between merocyanine and porphyrin dyes; porphyrin which is indirectly excited by the energy transfer is used as a light-electric energy photoconverter [180]. When a mixture of two good photoconverters (MgPC and MgTPP) is in PEC, the photocurrent intensity is much lower than that obtained in the presence of individual dyes. The decline in photoresponse is interpreted as related to high thermal relaxation of the aggregated dyes formed by the dyes in PEC [86,180,181]. However, the usefulness of larger arrays, including mixed systems with many components absorbing in the overlapped light range, was presented in [182]. Optimisation of light harvesting in porphyrin systems of highly ordered architecture in the form of columns kept by intermolecular  $\pi$ – $\pi$  stacking was shown [e.g. 183]. Photocurrent generation in a mixture of organic materials was also a subject of other investigations. A device with mixed solid of a weak electron-donating zinc porphyrin (5,10,15,20-tetra(2,5-dimethoxyphenyl)porphyrinatozinc) and a weak electron-accepting metal-free porphyrin 5,10,15-triphenyl-20-(3-pyridyl)porphyrin) was reported as a much better photosensitised cell compared to the cells with the pure individuals [184], resulting in photoinduced intramolecular electron transfer in a porphyrin heterodimer. An enhanced photocurrent was also observed for a Schottky-barrier cell with a mixed solid consisting of metal-free porphyrin and polythiophene compared to similar cells with monomeric porphyrin or pure polythiophene because of efficient cooperation of the hole and electron transports in the highly mobile polythiophene solid and the light harvesting porphyrin [177,185]. Platinum nanowires mixed with tin meso-tetra (4-pyridyl) porphyrin dichloride and Nafion were used to optimize photocurrent generation under irradiation with visible light [186,187]. An influence of dopa melanin

on photoresponses of charged tetraphenylporphyrins was also demonstrated [188]. Another interesting photocurrent responsive properties were investigated in porphyrin-containing conjugated polymers with, e.g. fluorine or carbazole as spacer groups and incorporation of carbazole units into the polymer chains was shown to give positive contribution to the photocurrent generation [189].

The third simple model of electron transfer from an excited dye to a semiconductor electrode as an acceptor is based on the use of porphyrin and quinone systems [69]. Photoinduced electron transport in a mixture composed of porphyrin ( $\text{H}_2\text{TPP}$ ,  $\text{MgTPP}$ ,  $\text{ZnTPP}$ ,  $\text{PbTPP}$ ) and anthraquinone (AQ) in DMSO by fluorescence and steady-state electron spin resonance (ESR) was also investigated [69]. The results show quenching of porphyrin dye fluorescence upon successive addition of AQ as an external quencher. The Stern–Volmer plots (Fig. 4.3a) confirm homogeneous dynamics of quenching of the porphyrin dyes by AQ [69,190]. The bimolecular quenching rate for metal-free and metal porphyrins ( $\text{H}_2\text{TPP}$ ,  $\text{MgTPP}$ ,  $\text{ZnTPP}$ ,  $\text{PbTPP}$ ) ranged from  $0.7 \times 10^{13}$  to  $13 \times 10^{13} \text{ M}^{-1} \text{ s}^{-1}$ . Fluorescence quenching in the presence of AQ was supposed to be induced by ET from porphyrin moieties to AQ; the ET rate constants were estimated as  $0.50 \times 10^9 \text{ s}^{-1}$  –  $\text{MgTPP}$ ,  $0.36 \times 10^9 \text{ s}^{-1}$  –  $\text{ZnTPP}$ ,  $4.17 \times 10^9 \text{ s}^{-1}$  –  $\text{PbTPP}$ . The light-induced ESR signals supported the thesis as to the origin of the unpaired electrons [69,191]. Analysis of the fluorescence results and ESR data (Fig. 4.3b) permits identification of the mechanisms responsible for the effects observed. The quenching of  $\text{PbTPP}$  fluorescence is faster than those of  $\text{MgTPP}$  or  $\text{ZnTPP}$ . The observed effects are discussed as resulting in ET but also in thermal relaxation and charge recombination processes [69,192]. A mixture of porphyrin derivative (tetrakis(4-N-hexadecylpyridiniumyl)) with AQ were also studied in a form of monolayers or Langmuir–Blodgett (LB) films [193]. However, the photocurrent in this mixture was lower than that in the photodevices based on LB films of the individual porphyrin due to incorporation of AQ. Examples of the energy and electron transfer in the systems composed of porphyrins (tetranaphthylporphyrin, tetraarylporphyrin) with different AQ derivatives as quenchers or porphyrin–AQ dyads bridged with a triazine group can be also found in [194–198]. Fluorescence quenching rate values [194] were evaluated in the similar way as it was done in [69] and it is postulated that quenching occurred as a result of formation of a charge transfer complex, [194,198]. There was also shown that there is no interaction between the ground-state porphyrin moiety and the ground-state anthraquinone one [69,194,195,198]. The quenching mechanism was interpreted as a static quenching with long-range dipole–dipole energy transfer between excited AQ molecules and the ground state of porphyrin and electron transfer from singlet excited state of porphyrin to AQ molecule and these lead to formation of radical ions [69,194–198].

Porphyrins and phthalocyanines were also studied by some authors in wide aspects of spectroscopic investigations and practical applications [e.g. 183,190,199]. Moreover, the effects of porphyrin substituents on photovoltaic properties of dyes have been also examined for a series of zinc meso-tetraphenylporphyrins sensitised in  $\text{TiO}_2$  cells [199]. It was shown that the cell photoactivity depends on the bridge between the porphyrin core and the  $\text{TiO}_2$  surface and its preparation procedure as well as the type of solvents. Photoinduced single-step ET on the nanometre scale in more complex systems like, e.g. strongly coupled zinc porphyrin–gold porphyrin dyad was also studied with the use of advanced methods to show the dynamics of the processes [81]. More complex objects like porphyrin–fullerene linked systems were also a subject of comprehensive study [e.g. 6,200]. The results provided by using the presented models have confirmed that conventional methods can be successfully applied to get data on photoinduced electron transfer processes.

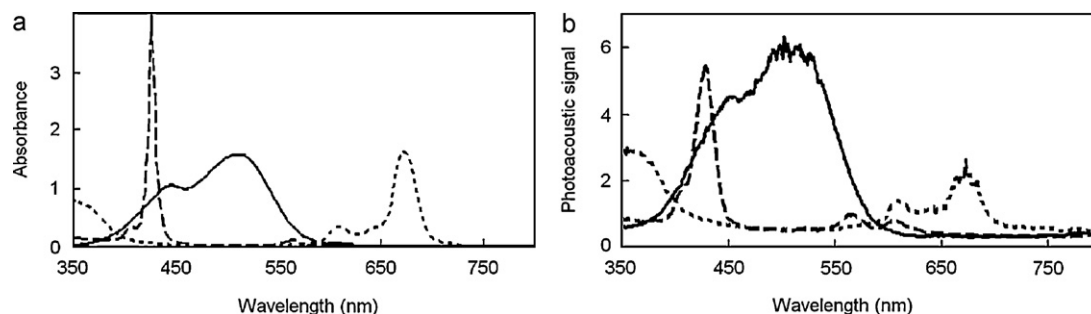


Fig. 4.2. Examples of the absorption (a) and photoacoustic (b) spectra of MgTNP (dashed line), SM (solid line), MgPc (dotted line) in DMSO.

#### 4.2. Fullerene–organic chromophore dyads, triads, tetrads

As mentioned above, the  $C_{60}$  molecule shows only four IR-active modes of the  $T_{1u}$  symmetry. However, in the  $C_{60}$  single crystal (fullerite) or in solutions of fullerene, the symmetry of the molecule should be reduced and the degeneracy of several vibrations should be lifted. Martin et al. [201] have observed over 180 vibrational absorption lines in the  $100\text{--}4000\text{ cm}^{-1}$  range. A similar effect was detected in a complex of  $C_{60}$  and chloro(triphenylphosphine)gold [202]. Over the past few decades, the intermolecular interaction of porphyrins and  $C_{60}$  has been studied extensively. Molecular mechanics calculations performed for various porphyrin–fullerene supramolecular complexes by Kang and Lin [203] have shown that porphyrin substituents introduce additional C–H (substituent)  $\cdots \pi$  (fullerene) interactions and enhance the interactions between porphyrin and fullerene species. Another interesting type of interaction is  $\pi$ – $\pi$  association between metalloporphyrins and  $C_{60}$ . Favourable van der Waals attractions between the curved  $\pi$ -surface of the fullerene and the planar  $\pi$ -surface of metalloporphyrin assist in the supramolecular recognition. This leads to complexes with contacts shorter than ordinary van der Waals ones and a variety of crystal structures [7]. However, the van der Waals force, very weak between porphyrins, plays a crucial role in formation of the most stable structures [203]. As it was mentioned before, to optimise intermolecular interactions the contact between fullerene and electron-donating molecule must be very close. The best way to optimise the contact between both moieties of the system is to induce covalent bonding of the parts. For construction of optoelectronic devices or artificial photosynthetic systems not only the interactions but also charge separation originating from photoinduced electron-transfer is of

utmost importance [5]. Imahori and his co-workers as well as other groups have found that  $C_{60}$  accelerates photoinduced charge separation and retards charge recombination in donor-linked  $C_{60}$  dyads [7,204–206]. On the other hand, porphyrins and fullerenes appear particularly suitable building blocks for construction of supramolecular systems displaying photoinduced energy and electron transfer processes [17,207–209].

A simple approach to forming of self-assembled supramolecular donor–acceptor dyads is the use of functionalised fullerenes in order to study light-induced electron transfer. The fullerene bears a nitrogenous ligand to coordinate the central metal of macrocyclic complexes such as porphyrin, phthalocyanine or naphthalocyanine. Complex formation can be confirmed by the UV–vis spectra (red shift of the Soret and Q bands), fluorescence (quenching of the steady-state fluorescence) and other techniques such as electron spray ionization mass spectroscopy, the  $^1\text{H}$  NMR spectroscopic measurements (appreciable upfield shift of the coordinated ligand) and molecular orbital calculations. The last methods are useful to arrive at optimized structures for the supramolecular conjugates and their electron structure [209–211]. The electron density of HOMO is localized in the porphyrin moiety while the electron density of LUMO is localized in the  $C_{60}$  moiety. This suggests that the most stable charge-separated state of the supramolecular dyad represented as  $C_{60}^{\bullet-} \rightarrow P^{\bullet+}$  [212] for the charge-transfer state having partial charge displacement in both HOMO and LUMO is represented as  $C_{60}^{\bullet\delta-} \rightarrow P^{\bullet\delta+}$ . Similar conclusion arises from *ab initio* and density functional theory calculations of Bhattacharya et al. [213]. For  $\text{H}_2\text{TPP}-C_{60}$  dyad LUMO, LUMO+1, and LUMO+2 are localized on the acceptor, whereas HOMO and LUMO+3 are localized on the donor side. However, for the  $\text{ZnTPP}-C_{60}$  dyad LUMO+1 and LUMO+2 are localized on the acceptor, HOMO and LUMO+3 – on the donor

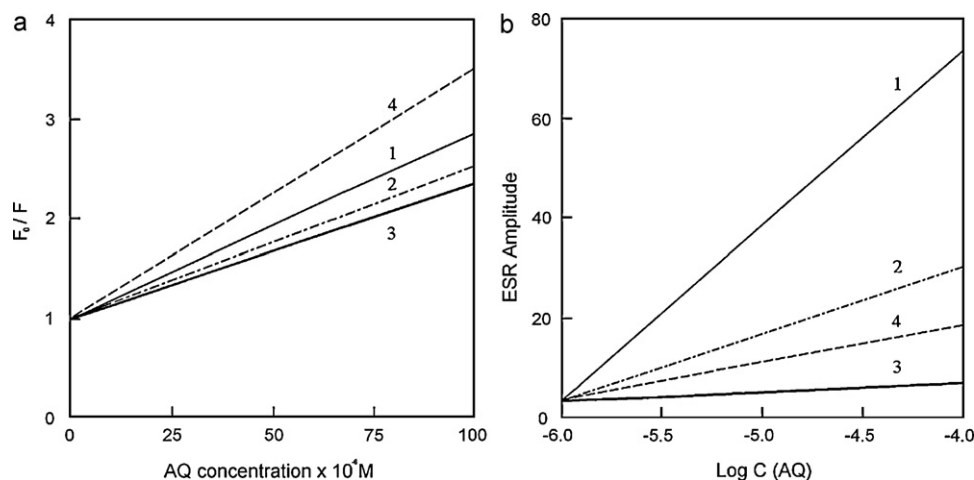


Fig. 4.3. Fluorescence ratio (a) and ESR amplitude of signals (b) of porphyrin–AQ mixture; MgTPP–AQ (1), ZnTPP–AQ (2), PbTPP–AQ (3),  $\text{H}_2\text{TPP}$  (4);  $F_0$  and  $F$  are the dye fluorescence intensities in the absence and presence of AQ.

side, whereas LUMO is partially localized on the acceptor and linker. Molecular electrostatic potential maps demonstrate the electron transfer phenomena from the porphyrin moiety to fullerene in both dyads [213].

Quantum chemical methods are also useful for molecular geometry optimization. The minimum energy indicates an optimal geometry of the molecular systems; it is also possible to find configurational and conformational isomers. For example, Herranz et al. using the semiempirical PM3 method have predicted the existence of two conformational isomers in C<sub>60</sub>-donor dyads in which the fulleropyrrolidine moiety is covalently attached to a  $\pi$ -extended tetrathiafulvalene analogue through an ethylenic spacer [214]. The donor fragment in this dyad is highly inclined from planarity. This is a consequence of the strong steric hindrances between the sulfur atoms of the dithiol rings and the CH units in *peri* positions. Theoretical calculations predict a higher stability of the trans isomer with two dithiol rings pointing upwards [214].

As mentioned above, fluorescence spectroscopy can confirm complex formation. As was shown by El-Khouly et al. addition of fullerene to porphyrin in toluene solution decreases the fluorescence intensity to about 30% of the original intensity [215]. It is well known that in porphyrin–fullerene systems the charge-separated state is formed in polar solvents *via* photoinduced electron transfer. However, some systems produce the charge-separated states even in nonpolar solvents. Numerous laboratories investigate systematically solvent dependent change in the charge separation and recombination processes. Photodynamic processes have been usually studied by fluorescence lifetime measurements. For example, the fluorescence lifetimes of the typical dyad zinc porphyrin–fullerene were measured by a time-correlated single photon-counting apparatus with excitation at 410 nm, and monitored emission originated from the porphyrin and fullerene moiety at 610 and 720 nm, respectively [216]. The fluorescence lifetimes of the dyad at 610 nm (in nonpolar solvents) are much shorter than those of zinc porphyrin. On the other hand, the lifetime of the excited state absorbing at 720 nm in the dyad becomes longer when the solvent polarity decreases, approaching the lifetime of C<sub>60</sub>. All these and other experimental observations suggest that the charge-separated state in benzene, produced *via* photoinduced electron transfer, undergoes charge recombination to yield C<sub>60</sub> [216–218]. Electron transfer dynamics can be rationalized by the small reorganization energy of porphyrin–fullerene systems – such information is helpful for developing artificial photosynthetic systems. To have this subject in view, a new group of porphyrin–fullerene dyads with an azobenzene linker was synthesized [219]. The photophysical and photochemical properties of these materials were investigated using steady-state and time-resolved spectroscopic methods. While no major differences were observed in the rate constants of photoinduced intramolecular electron transfer in comparison with closely analogous dyads with amide and acetylenic linkers, the back electron transfer rates was significantly faster in the azo-linked dyads. In all cases, the rates of back electron transfer are slow relative to the rates of charge separation, by as much as 4 or 5 orders of magnitude [219]. Lemmetyinen et al. have synthesized selected phthalocyanine–fullerene dyads [220]. These dyads have different orientations of phthalocyanine and fullerene, which strongly influence the electron transfer from phthalocyanine to fullerene moiety. Fluorescence quenching of the dyads were measured in both polar and nonpolar solvents, and in all cases, the quenching was more efficient in the polar environment [220]. The same group had studied the photoinduced electron transfer in five structurally different phytychlorin–fullerene dyads [221]. The dyads have been studied in polar and nonpolar solvents using femtosecond fluorescence up-conversion and pump-probe transient-absorption techniques. Small changes in the structures of the dyads result in considerable changes in the electron transfer properties [221]. The first excited

singlet state of phytychlorin is in equilibrium with an intramolecular exciplex state. In polar solvent the exciplex undergoes an electron transfer, and a complete charge separated state is formed with the quantum yield close to unity. The phytychlorin–fullerene dyads form the complete charge separated state also in nonpolar solvent with the yield influenced by minor changes in the molecular structure. These new dyads have a weaker phytychlorin–fullerene interaction due to longer separation distances between the two moieties and therefore the energies of exciplex states are increased, and thus their formation rates are reduced [221]. The most compact structure of the donor–acceptor pair may not be optimal from the point of complete charge separation.

In this chapter we would like also to recapitulate our recently performed investigations of molecular and electronic structure as well as electronic and vibrational excitations of fullerene derived systems containing organic chromophores such as modified porphyrins, diimide-derivatives, thiophene-based systems and so on; all these molecules strongly absorb sunlight and can play a role of electron donors in photovoltaic systems [202,222–227]. Physical properties of the dyes, in particular their electron and vibrational structure, depend on the molecular geometry of the compounds. The most probable molecular configuration of porphyrin or other organic chromophore dyads with fullerenes can be found by calculations with the use of Gaussian 03 program [228]. According to our calculations, the phenyl groups assume positions perpendicular to the porphyrin plane in the spatially most convenient conformation D<sub>4h</sub> of TPP. However, a low-symmetry arrangement can be also possible. For the C<sub>1</sub> symmetry, the independent motion of the Ar group can stabilize the structure. In fact, for this symmetry, the bonding energy of the molecule shows a minimum. The optimal angles between the phenyl groups and the porphyrin plane for S<sub>4</sub> symmetry are  $\pm 62^\circ$  but for C<sub>1</sub> – between 62 and 65° [224]. The structure of TPP of the symmetry D<sub>4h</sub> and C<sub>1</sub> and the structure of its dyad with fullerene are shown in Fig. 4.4a and b.

In the fully optimised geometry of the zinc porphyrin dimer the angle between the porphyrin planes of the monomers is 88°, whereas the distance from the centre to centre of the monomers (Zn–Zn distance) is 8.39 Å (Fig. 4.4c).

Typical vibrational spectra of the fullerene–porphyrin dyad are discussed taking into consideration the results of our study of the dyad consisting of the zinc *meso*-tetraphenyl porphyrin scaffold with C<sub>60</sub> moiety attached to the short pyrrolidine single linker [224]. IR absorption spectra of the dyad, the zinc *meso*-tetraphenylporphyrin and the modified fullerene with a linker are shown in Fig. 4.5.

Most of the bands attributed to the vibrations of porphyrin can be found in the spectra of the dyad at the same or slightly shifted frequencies. Similar vibrational spectra of various porphyrins and the band assignments have been reported in literature [229–231]. The shape of some bands of the dyad is changed in comparison with that in the corresponding region of the porphyrin spectra. For example, the C=C and C–C stretching modes of porphyrin occurring at 1476 and 1497 cm<sup>−1</sup> appear as a double band with maxima at 1476 and 1495 cm<sup>−1</sup> in the spectrum of the dyad. We conclude that the formation of the fullerene–porphyrin dyad causes small changes in the electron distribution on the porphyrin moiety, which affect its vibrational force constants observed as small shifts of the band position [224].

Four bands at 527 (very strong and narrow), 575, 1179 and 1425 cm<sup>−1</sup> were observed in the IR spectrum of the dyad studied. The bands at 527 and 575 cm<sup>−1</sup>, which also appear for pristine C<sub>60</sub> and the modified fullerene, correspond to T<sub>1u</sub> modes related to radial deformation of the fullerene moiety [232]. The frequencies of these vibrations are unchanged upon formation of the dyad. The two remaining IR-active bands of C<sub>60</sub>, which are related to its tangential deformations [232], are located at 1182 and 1428 cm<sup>−1</sup>.



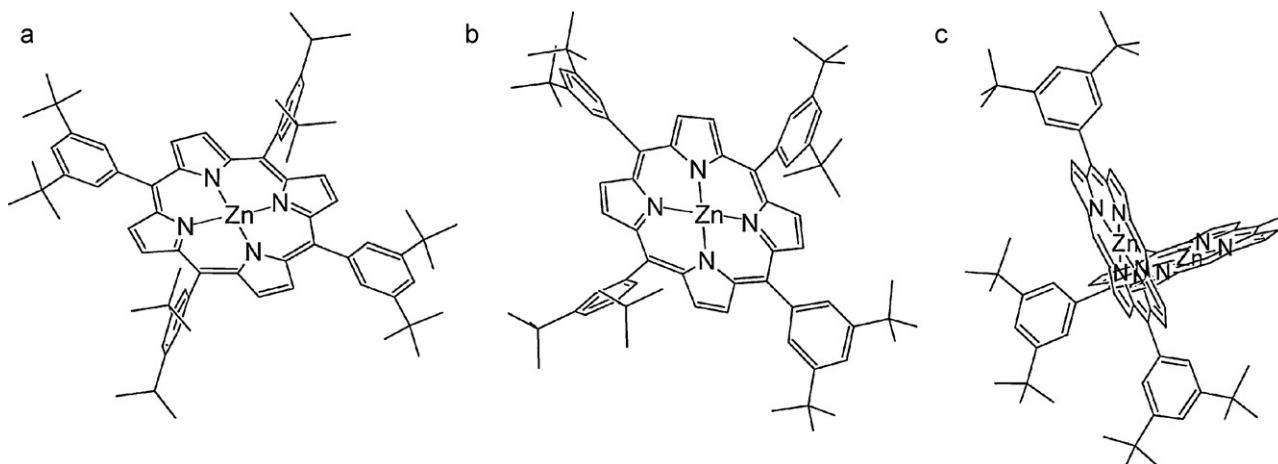


**Fig. 4.4.** Molecular structure of the 5,10,15,20-tetrakis(3,5-di-tert-butylphenyl)porphyrinatozinc(II) (TBPP) of the  $D_{4h}$  (a) and  $C_1$  (b) symmetries and its dimer structure (c).

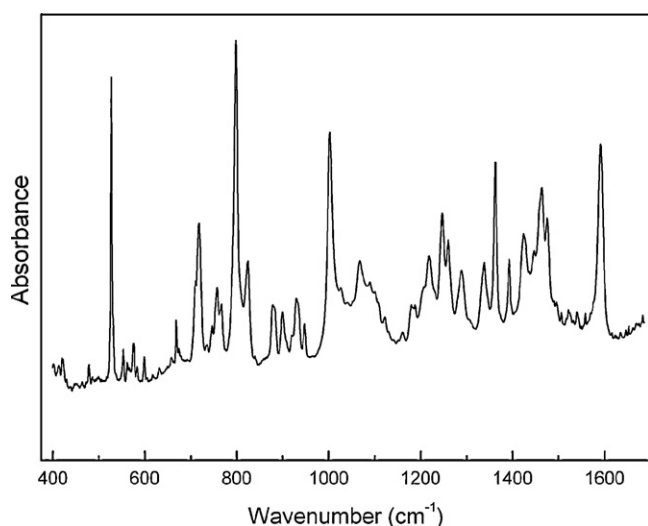


**Fig. 4.5.** IR absorption spectrum of TPP- $C_{60}$  dyad recorded in KBr pellet, at room temperature.

The tangential modes of the fullerene would undergo small, about  $3\text{ cm}^{-1}$  shift and line shape deformation after functionalization of the  $C_{60}$  molecule. Similar effects were also observed for other such dyads such as [60]fullerene-TTF [233], *meso*-linked oligoporphyrin

bearing one or two fullerene moieties [14] and [60]fulleropyrroli-  
dines [234]. It seems that the tangential deformations of  $C_{60}$ ,  
in contrast to the radial deformations, are distinctly perturbed in  
modified fullerenes [224]. Electronic spectra of the dyads contain-  
ing  $C_{60}$  and various porphyrin-derived dyes are collected in Fig. 4.6.  
Three strong absorption bands identified as the dipole-allowed  
transitions in pristine  $C_{60}$  are observed at 206, 264, and 340 nm  
[223]. The electronic spectrum of the zinc porphyrin is dominated  
by the very strong Soret band located at 420 nm (Fig. 4.6a).

Contrary to the porphyrin molecule, the spectrum of porphyrin  
dimer shows a splitting of the Soret band into a doublet at 416 and  
452 nm (Fig. 4.6b). This suggests that the second singlet-excited  
states of both porphyrin units are coupled leading to the splitting  
of the singlet electronic levels. The Soret absorption band in the  
spectrum of fullerene-porphyrin dyad is bathochromically shifted  
from 420 to 430 nm testifying to the electronic interaction between  
porphyrin dye (electron donor) and fullerene acting as an electron  
acceptor. In contrast to the bands characteristic of the porphyrin  
scaffold, the bands of the fullerene moiety, in particular those at  
264 and 340 nm, undergo small hypsochromic shifts. In spite of the  
covalent linkage and vicinity of both fullerene and porphyrin  $\pi$ -  
systems, the observed spectroscopic changes are probably related  
to both through-band and through-space electronic interactions  
between the fullerene and appended chromophores. The Soret dou-  
blet in dyads containing the porphyrin dimer is bathochromically  
shifted when compared to the doublet in the spectrum of the por-

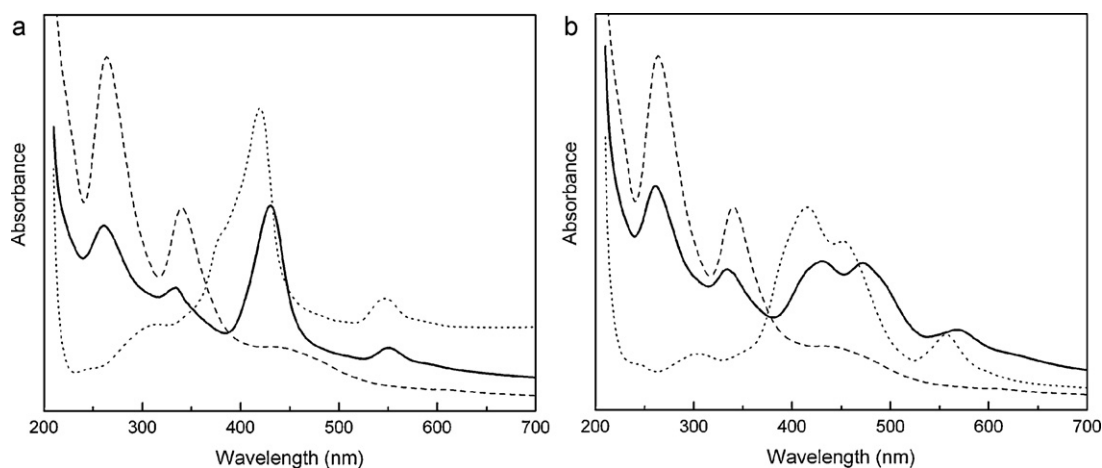


**Fig. 4.6.** Electronic absorption in KBr pellets at room temperature of fullerene-porphyrin dyad and the dyad components:  $C_{60}$  – dashed line, P – dotted line, P- $C_{60}$  – solid line (a) and the spectra of the dyad fullerene-porphyrin dimer and its components  $C_{60}$  – dashed line, 2P – dotted line, 2P- $C_{60}$  – solid line (b).



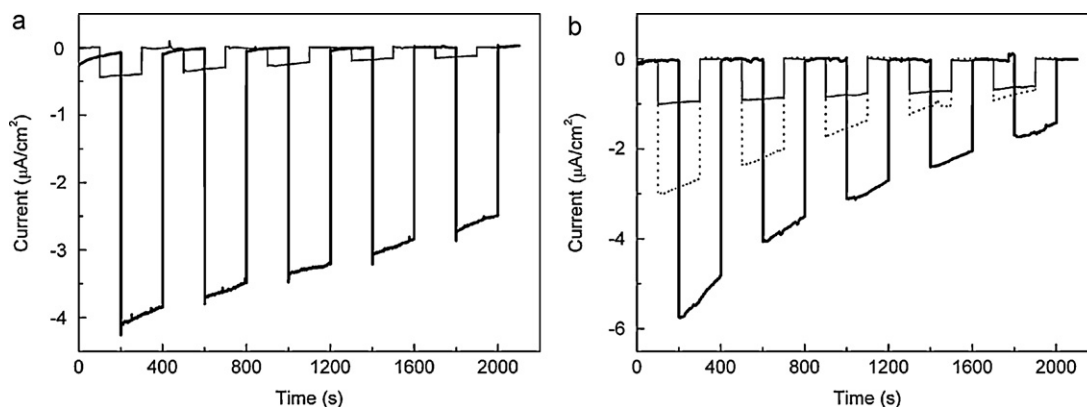


**Fig. 4.7.** Photocurrent of the porphyrin–fullerene systems; 1P – solid line, 1P-C<sub>60</sub> – thick solid line (a) and 2P – dotted line, 2P-C<sub>60</sub> – solid line, 2P-2C<sub>60</sub> – thick solid line (b).

phyrin dimer. The doublet at 416 and 452 nm in the spectrum of the dye is shifted to 426 and 465 nm in that of the dyad; this shift is more distinct if two C<sub>60</sub> molecules are bonded to the porphyrin dimer (431 and 472 nm, respectively) [226]. The absorption bands of both moieties of the dyads are not only shifted but also are distinctly broadened. These effects testify to the fact that the electron distribution is significantly changed after the dyad formation.

Strong interaction in the porphyrins covalently linked to C<sub>60</sub> was also studied by the fluorescence, PAS and LIOAS methods [117,225]. Results obtained with these methods not only confirmed that the presence of fullerene influences markedly photophysical properties of fullerene–porphyrin dyads because of strong interaction between fullerene and covalently linked chromophore, but provide the evidence for intramolecular energy transfer from fullerene to porphyrin. Strong interactions in the systems under studies lead not only to charge redistribution but also creation of excimers [117,225]. The LIOAS study permits determination of the basic parameters such as quantum yield of triplet states population and thermal relaxation decay of triplet states which are very important in molecular photovoltaics. All these data are useful in designing molecular light converting systems. Charge redistribution and localization of electrons were studied by ESR [227,235]. The light-induced ESR signal was found to increase stepwise with the incident light and decrease very slowly when the light was switched-off. The detailed resonance studies revealed that the main ESR parameters of porphyrins are weakly dependent on the number of porphyrin molecules and these parameters are not noticeably changed after the dyad formation [227]. The electron–donor–acceptor character of the systems under studies was also confirmed by examination of photocurrent generated in a photoelectrochemical cell composed of gold and semiconductor electrodes. The LB films of the porphyrin–fullerene dyads showed the most intensive cationic current when the photoelectrochemical cell was sensitised by porphyrin–fullerene system [200]. The enhanced photoresponse was received in PEC with the ZnP–C<sub>60</sub> system due to slowing down a charge separation process. When the cell is filled with porphyrin dyads with fullerene also thermal deactivation has to be considered as a reason for photosignal reduction [200]. Results of the photocurrent measurements of the porphyrin–fullerene systems are shown in Fig. 4.7a and b.

In the majority of donor–fullerene linked systems constructed with the use of symmetric tetrapyrroles such as porphyrin and phthalocyanine, it was difficult to probe a slower charge recombination process. Thus, it is desired to develop donor–acceptor dyads which can afford long-lived charge-separated states [236]. One possibility is to replace these symmetric donors with, e.g. corroles [237]. Corroles are one-carbon-shorter analogues of porphyrins possessing the skeleton of corrin with three *meso*-carbons between the four pyrrole rings [236]. Recent synthetic breakthroughs have

made these macrocycles more available [238,239]. When compared to porphyrins, these tribasic aromatic macrocycles exhibit lower oxidation potentials, higher fluorescence quantum yields, larger Stokes shifts, and more intense absorption of red light [240,241]. The first example of covalently linked free-base corrole–fullerene dyads was reported by D'Souza et al. [236]. Corrole–fullerene dyads reveal an absorption band around 310 nm. The Soret band of the dyad is blue-shifted by 5 nm compared to the reference corrole; such a trend is observed for Q bands around 560 nm. These shifts suggest electronic interactions between the corrole and fullerene entities of the dyad. The HOMO state is located mainly on the corrole  $\pi$ -system, but it is also on a spacer of the dyad whereas LUMO is located on the fullerene spheroid [242]. The locations of HOMO and LUMO suggest formation of the corrole<sup>+</sup>–C<sub>60</sub><sup>−</sup> charge-separated state during photoinduced electron transfer [236]. Free-base corroles reveal an emission band at 656 nm with a shoulder around 714 nm but in the dyad this emission is fully quenched [243]. This result indicates efficient excited-state events in the dyad. The rate constant of charge separation ( $k_{CS}$ ) is between  $10^{10}$  and  $10^{11}$  s<sup>−1</sup> but the quantum yield ( $\Phi_{CS}$ ) is found to be >97% [236]; it suggests an efficient photoinduced electron transfer process.

Molecular systems designed to mimic the photosynthetic reaction centre must exhibit a preference for electron transfer over energy transfer at longer distances since the energy transfer rate decreases rapidly with increasing distance between the donor and acceptor [7,244,245]. Yamada et al. [246] have proposed to incorporate a “molecular wire” in the D–A system to facilitate electron transfer over long distances. Linear  $\pi$ -conjugated polyene and polyyne spacers enhance through-bond electronic coupling between D and A [247]. Thus, systems in which the redox centres are separated by such “molecular wires” exhibit efficient long-range electron and energy transfer. The porphyrin–fullerene dyad, in which the chromophores are conjugatively linked through a butadiyne “molecular wire”, was synthesised and described few years ago [248] – it seems that the butadiyne-linked dyad is a prototype of a new family of photoactive materials. Small red shifts apparent in the UV–vis absorption spectra of the dyad relative to the porphyrin do not provide any evidence for a ground-state interaction between the two  $\pi$ -systems. On the other hand transient absorption studies show that the efficient quenching of porphyrin fluorescence by the attached fullerene moiety in the molecular wire is due to photoinduced electron transfer to give a charge separated state P<sup>+</sup>–alkyne–C<sub>60</sub><sup>−</sup> [248]. The fluorescence lifetime measurements support the notion that the triple bond is a very efficient mediator of electronic interaction between porphyrin and fullerene moieties.

Recently, the thiophene oligomers and thiophene-derived systems have been widely studied experimentally and theoretically. For example, we studied the vibrational and electronic properties

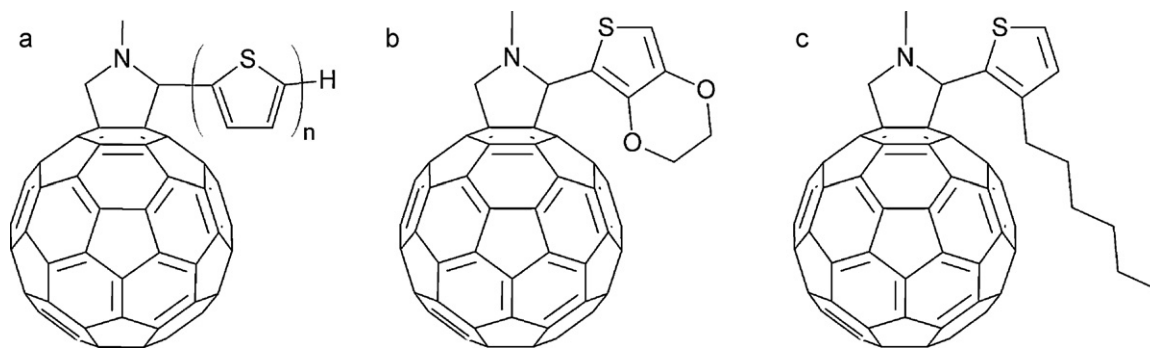


**Fig. 4.8.** Chemical structure of the thiophene-based fullerene dyads: oligothiophene–fullerene dyads with  $n=1, 2$ , and  $3$  (a), dyad of ethylenedioxythiophenyl (EDOT)–fullerene (b), and dyad of hexylthiophenyl (HXT)–fullerene (c).

of selected oligothiophene–fullerene and thiophene-derivative–fullerene dyads by electronic and infrared absorption as well as Raman scattering methods [249,250]. Spectroscopic investigation was supported by quantum chemical simulations of the molecular structure, normal mode vibrations and electron levels of the dyads. Chemical structure of the thiophene-based fullerene dyads are shown in Fig. 4.8. The experimental electronic spectra of all dyads investigated recorded in KBr pellets are presented in Fig. 4.9. The spectra of the dyads are similar to each other and dominated by the bands characteristic of the fullerene molecule. However, there are some differences related to the changes in the molecular geometry of the dyads. A singular observation was the additional broad band observed at about 393 nm in the spectrum of fullerene–oligothiophene (for  $n=3$ ; 3T- $C_{60}$ ) dyad [249,250].

For understanding these differences, the time dependent density functional theory (TD-DFT) calculations of transition energies were performed for all the dyads [249]. The results are shown in Fig. 4.10. In most of investigated molecular orbitals, the electron density is localized completely on the one of the moieties: fullerene or thiophene-derived units. Almost all HOMO and LUMO orbitals in the compounds investigated are localized on the fullerene moiety but for 3T- $C_{60}$ , the HOMO orbital is localized only on the oligothiophene part while LUMO is located on the fullerene part [249].

The energy gap between HOMO and LUMO is similar in all investigated thiophene-derived materials. Usually, the gap  $\Delta_{H-L}$  is of about 2.55 eV, but in the 3T- $C_{60}$  dyad the gap is signif-

icantly lower ( $\Delta_{H-L}=2.26$  eV). Supplementary calculations gave the energy gap of  $\Delta_{H-L}=2.07$  eV for 4T- $C_{60}$  dyad. These differences were related to the length of the oligomer and probably to the electron delocalization connected with that length [249]. The above mentioned observations suggest that the way to improve the intramolecular charge transfer in the materials of this type is to use longer oligothiophene or similar molecule/group linked to the fullerene. However, it seems that in the dyads containing thiophene-derived molecules the crucial is not the length of the donor moiety but the presence and number of rings in its chemical structure. Vibrational properties of various dyads containing oligothiophenes or thiophene-derived molecules and fullerene have been widely described by Barszcz et al. [249]; Fig. 4.11 shows these results. It has been also proved that changes in the molecular structure of the dye lead to specific changes in the spectra of corresponding dyads.

Another interesting chromophore for various applications is perylene-3,4:9,10-tetracarboxydiimides (PDI). It was recently linked to fullerene  $C_{60}$  with the aim of inducing intramolecular energy transfer and enhancing the efficiency of organic solar cells [251,252]. We have been interested in development of a dissymmetrical PDI building block in order to investigate its grafting to both  $C_{60}$  and tetrathiafulvalene to obtain PDI- $C_{60}$  and PDI-TTF dyads.

The UV–vis spectra of these dyads are shown in Fig. 4.12. The absorption bands of the fullerene moiety are broadened and shifted; the band at 334 nm undergoes a hypsochromic shift by 9 nm compared to the wavelength of the respective band of  $C_{60}$  [141]. Some perylenediimide absorption bands show bathochromic shifts by a few nanometres (on average 7 nm) with regard to the components of the triple absorption of PDI. The absorption spectrum of PDI-TTF resembles that of PDI, that means that TTF does not change significantly the electronic structure of the chromophore.

On the basis of results of the spectroscopic studies of the dyads of fullerene–organic chromophore presented above and taking into account extensive literature data, we can conclude that various spectroscopic methods such as infrared and electron absorption spectroscopy, Raman scattering and others can be successfully used for characterisation of such complex molecular systems as fullerene–organic chromophore dyads.

#### 4.3. Branched donor–acceptor ensembles and self-organised systems

Application of fullerenes in multistep electron transfer systems seems to be the next step towards improvement of solar energy conversion devices. There are a lot of reports about triads, tetrads, pentads and others containing organic chromophore and fullerene [84,206,224,253–255].

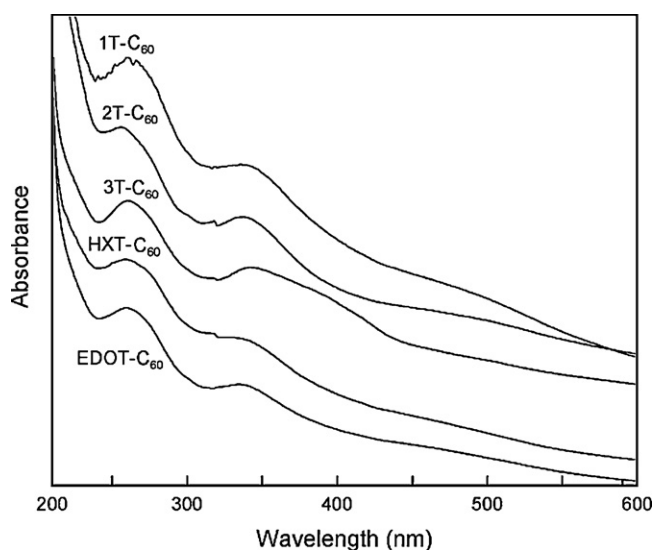


**Fig. 4.9.** Experimental electronic spectra of the investigated dyads recorded in KBr pellets. For clarity of the figure the absorbance scale is not preserved.

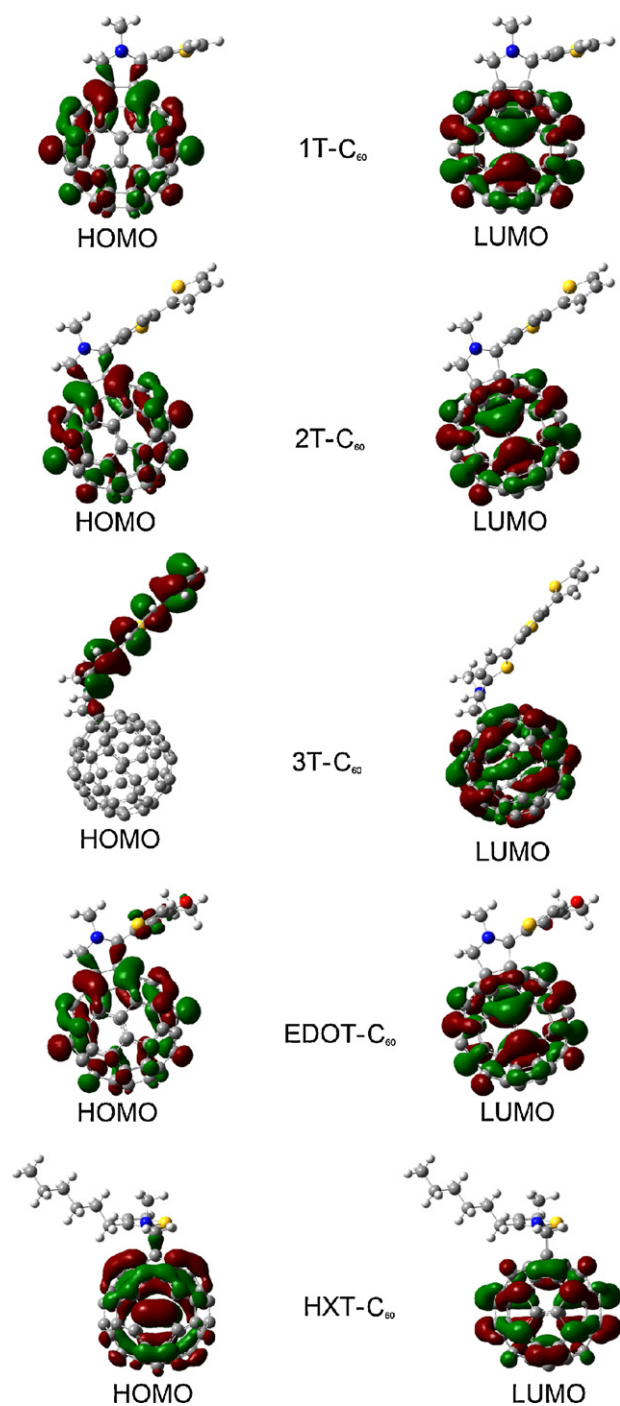


**Fig. 4.10.** The contour plots of the highest occupied molecular orbitals (HOMOs, left side) and the lowest unoccupied molecular orbitals (LUMOs, right side) of the investigated dyads fullerene–thiophene.

In this chapter we concentrate on photophysical properties of porphyrin–organic donor molecule–fullerene triads and tetrads, *e.g.* porphyrin–pyromellitimide–fullerene [82,224] or ferrocene–porphyrin–fullerene [82,256]. An additional donor, *i.e.* ferrocene, was attached to the porphyrin–fullerene dyad to prolong the lifetime of the charge-separated state without lowering the charge separation efficiency. One of the first porphyrin–fullerene-linked tetrad was ferrocene–zinc porphyrin–free base porphyrin–fullerene (Fig. 4.13a) synthesized by Imahori *et al.* [216]. Guldi [7] and Imahori [216,255] investigated the lifetime of the charge separated state *via* systematic

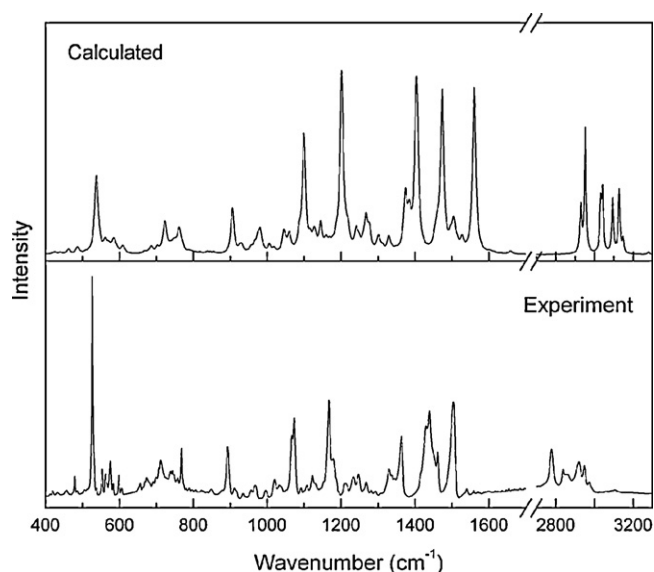


**Fig. 4.11.** Experimental IR absorption spectrum of the dyad EDOT–C<sub>60</sub>, with adequate calculated spectrum obtained with theory level B3LYP/6–31G(d,p).

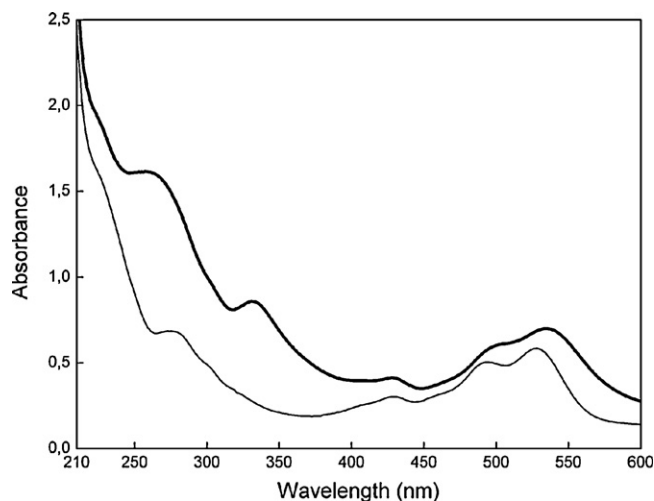


**Fig. 4.12.** UV–vis spectra of the dyads PDI–C<sub>60</sub> (thick solid line) and PDI–TTF (solid line).

extension of the donor–acceptor composition. It was shown that a donor–acceptor distance and long-lived charge separated state can only be attained in a series of short-range, fast and efficient electron transfer systems if wire-like spacer units are employed [7]. Porphyrin–fullerene-linked triads and tetrads display stepwise electron transfer relay, mimicking the primary charge separation in the photosynthetic reaction centre. Long-lived charge-separated state up to 16  $\mu$ s and highly efficient electron transfer were observed in the ferrocene–zinc porphyrin–fullerene triad [5]. The lifetime of the charge-separated state in the ferrocene–zinc porphyrin–free base porphyrin–fullerene tetrad is 0.34 s in benzonitrile [5]. It seems that more elaborate porphyrin–fullerene-linked systems will be the next step for obtaining high quantum yield of charge separation and the lifetime of the charge-separated state longer than in natural systems.

Another promising approach for achieving good structural control and light-harvesting properties is the self-assembly of dye or dye–fullerene systems. Molecular self-assembly processes lead to the construction of large and ordered superstructures by the use of weak, noncovalent bonding interactions between complementary

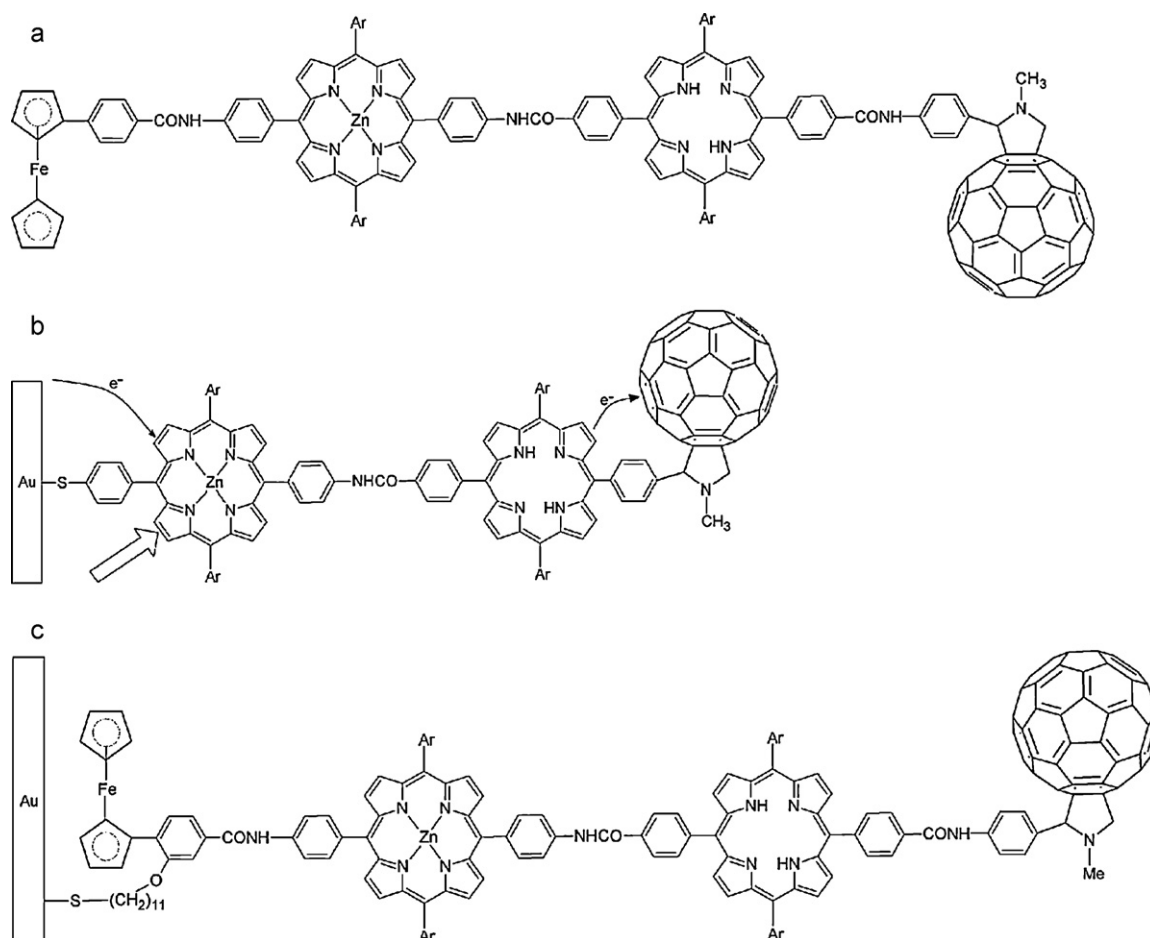


**Fig. 4.13.** Scheme of the molecular structure of ferrocene–zinc porphyrin–free base porphyrin–fullerene tetrad (a), photoinduced multistep electron transfer at gold electrode modified with self-assembled monolayer of porphyrin–C<sub>60</sub> sulfide (b), and photoinduced multistep electron transfer at gold electrode modified with self-assembled monolayer of ferrocene–porphyrin–C<sub>60</sub> alkanethiol (c).

molecular structures [257–259]. The first porphyrin–fullerene-linked dyads containing zinc porphyrin and porphyrin without metal at the centre, in self-assembled monolayers were reported by Imahori et al. [260]. Since sulfides are relatively stable components, a methylthio group was attached to one end of a porphyrin ring, while the opposite end had a C<sub>60</sub> moiety (Fig. 4.13b). Extended spectroscopic investigation of the self-assembled monolayers of zinc porphyrin–C<sub>60</sub> dyad/Au and free-base porphyrin–C<sub>60</sub> dyad/Au (where/represents an interface) revealed that the porphyrin–C<sub>60</sub> molecules are tilted nearly parallel to the gold surface, leading to the formation of loosely packed structures [5]. Under short-circuit conditions, cathodic photocurrent was observed in the photoelectrochemical system with the quantum yield 0.5% [5,260]. Self-assembled monolayer systems of the porphyrin–fullerene-linked dyads have been extended to porphyrin–fullerene triads with an alkanethiol [261]. The alkanethiol-attached triads involve a linear array of ferrocene–porphyrin–fullerene. When a thiol group is introduced at the end of the donor–acceptor-linked molecules, it is arranged unidirectionally at the gold electrode, leading to formation of a uniform self-assembled monolayer with a thickness of about 50 Å (Fig. 4.13c). The triad molecules are well-packed with an orientation almost perpendicular to the gold surface [5,256]. The mixed self-assembled monolayers on the gold electrode have enabled a cascade of photoinduced energy transfer and multistep electron transfer, leading to the production of photocurrent output with the highest internal quantum yield ever reported for photocurrent generation at monolayer-modified metal electrodes [257].

Recently, the photoinduced electron transfer processes in supramolecular fullerene systems with various electron donors have become the most investigated phenomena. Huge amount of new self-assembled supramolecular triads, tetrads, pentads and larger molecular systems have been formed *via* metal–ligand coordination, crown-ether inclusion, ion pairing, hydrogen bonding, or  $\pi$ – $\pi$  stacking interactions. Although the single mode of binding gives flexible supramolecular structures, the newly developed strategy of multiple modes of binding results in conjugates of defined distances and orientation between the donor and acceptor entities, which influences the overall electron transfer reactions [209]. In these conjugates an acceleration of the charge separation process and deceleration of the charge recombination are observed. However, studies on these self-assembled supramolecular systems anticipate involvement of more complex systems for better performances in light-driven devices, in particular in the field of photovoltaics [209,262].

For example, ferrocene–phthalocyanine–fullerene supramolecular triads were constructed with pyridine or imidazole appended fulleropyrrolidene and covalently linked zinc phthalocyanine–ferrocene dyad *via* axial coordination [263]. Steady-state and time-resolved fluorescence measurements performed by Zhao et al. [263] shown the occurrence of efficient photoinduced electron transfer from excited phthalocyanine to fullerene entity in the triad with  $k_{CS} = 10^9 \text{ s}^{-1}$  and with high charge-separation quantum yields  $\varphi_{CS} = 0.88$ . The formation of a long-lived charge-separated state of self-assembled donor–acceptor tetrad obtained by axial coordination of a fulleropyrrolidene appended



with an imidazole coordinating  $C_{60}$  ligand to the zinc centre of a subphthalocyanine–triphenylamine (TPA)–ZnP was recently investigated [264]. The majority of the highest occupied frontier molecular orbital was found over the ZnP and TPA entities, whereas the lowest unoccupied molecular orbital was located over the fullerene entity, suggesting the formation of the radical–ion pair. The femtosecond transient absorption measurements revealed fast charge separation from the singlet porphyrin to the coordinated  $C_{60}$  with the life-time of 1.1 ns; slow charge recombination ( $1.6 \times 10^5 \text{ s}^{-1}$ ) and the long life-time of the charge-separated state (6.6  $\mu\text{s}$ ) were observed in toluene [264]. A self-assembled supramolecular triad where boron dipyrin, zinc porphyrin, and fullerene respectively constitute the energy donor, electron donor, and electron acceptor segments of the system was studied recently [265]. Selective excitation of the boron dipyrin moiety in the dyad results in energy transfer over 97% efficiency creating singlet excited zinc porphyrin. Upon forming the supramolecular triad by self-assembling fullerene, the excited zinc porphyrin resulted in electron transfer to the coordinated fullerene, yielding a charge-separated state. Nanosecond transient absorption studies permitted to evaluate a lifetime of the charge-separated state to be 23  $\mu\text{s}$ , indicating charge-stabilization in the supramolecular triad [265]. Supramolecular triads of free-base porphyrin, fullerene, and ferric porphyrin were characterised by spectroscopic methods and deduced from quantum chemistry calculations [266]. Free energy calculations and emission data suggested the occurrence of sequential electron transfer from singlet excited free-base porphyrin to the covalently linked fullerene, followed by an electron transfer from fullerene anion radical to ferric porphyrin, generating free-base porphyrin cation radical and ferrous porphyrin as the electron transfer products. It anticipates generation of long-lived charge-separated species as a consequence of distance separation between the oxidized and reduced species [266]. Lifetimes of the final charge separated species of the order of 20  $\mu\text{s}$  were obtained. The dramatic changes of the lifetimes of the charge separated states were also observed in ZnP–oligothiophene (nT)– $C_{60}$  linked triads with the solvent polarity [267]. The energy transfer mechanisms were described in details in the paper of Nakamura et al. [267]. The relationship between the energy levels of two charge separated states, which strongly depends on the solvent polarity, causes large changes of the lifetime of the charge separated state in ZnP–nT– $C_{60}$ . The longest lifetime of the charge separation states of 450–910  $\mu\text{s}$  was detected in o-dichlorobenzene; it is about 30 times longer than those in  $H_2P$ –nT– $C_{60}$  in the same solvent [267].

It is necessary to add, that extension of the self-assembly approaches to single wall carbon nanotubes results in nanotube-porphyrin/phthalocyanine nanohybrids capable also of undergoing photoinduced electron transfer [261].

#### 4.4. Molecular arrangement in Langmuir–Blodgett films

The structure, formation and molecular organisation (including orientation of planar fragments of molecules) of organic layers are the subjects of current interest. Various spectroscopic methods are excellent techniques of probing surfaces and interiors of thin films because they give fundamental information on the properties of systems minimizing destruction of the sample as compared to a number of other film analysis methods. Now, spectroscopic methods are commonly used for quantitative determination of molecular organisation in multilayered thin organic films of potential application in photovoltaics [268–278]. This subject was also of interest to us [200,279–282].

In particular optical ellipsometric spectroscopy [283,284], infrared reflection or reflection–absorption (IRRA) spectroscopy [275–277,285], Raman spectroscopy [286], as well as X-ray reflec-

tivity [287] and fluorescence spectroscopy [288] are the most useful techniques for determination of molecular orientation in the films.

Molecular arrangement in LB layers can be evaluated from the polarized spectra in the visible range. Under supposition of the flat  $\pi$ – $\pi^*$  molecular structure of the organic chromophore and when the layer is illuminated with the polarised light, dichroism of the film can be expressed as:

$$D_\beta = \frac{A_1}{A_2}$$

where  $A_1$  and  $A_2$  are the film absorbances for polarized light with the electrical vectors parallel and perpendicular to the film dipping direction, respectively. The dichroic ratio is a function of  $\Phi$ ,  $\theta$ , and  $\beta$  angles determining an orientation of the flat molecule in the Cartesian space. Yoneyama et al. [289] have introduced a parameter  $P_x$  corresponding to the fraction of molecules with the centre axis  $z'$  projections parallel to the Cartesian  $x$  axis:

$$P_x = \frac{\langle \sin^2 \theta \cos^2 \Phi \rangle}{1 - \langle \cos^2 \theta \rangle}$$

where  $\langle \rangle$  denotes a statistical average. This parameter is limited to  $0 < P_x < 1$ . It means that when  $P_x > 0.5$  a ring face is oriented preferably to the  $x$  axis, and to the  $y$  axis when  $P_x < 0.5$ . This method was used by us for study the molecular arrangement of selected porphyrin and phthalocyanine dyes [272].

The orientation of organic molecules grafted to a metal surface can be also determined using IRRA spectroscopy. Each molecular vibration is characterized by the transition dipole moment  $M$  which can be decomposed into components normal ( $M_z$ ) and parallel ( $M_x$ ) to the metal substrate. At the metal surface the electric field component  $E_x$  of the incident electromagnetic wave is screened by the electrons of the metal substrate and the  $M_x$  component does not contribute. Therefore, for a single vibrational mode, the tilt angle can only be determined if the absolute magnitude of  $M$  is known [277]. The situation is improved if two vibrational modes ( $i$  and  $j$ ) of different orientations of their transition dipole moments can be measured. Taking into consideration that the intensity of the band  $I^{\text{bulk}}$  recorded for the bulk spectrum (e.g. in KBr pellet) is proportional to the square of adequate transition dipole moments  $M$  of the band ( $I^{\text{bulk}} \sim M^2$ ), the ratio of two bands intensities can be expressed by equation:

$$\frac{I_i^{\text{bulk}}}{I_j^{\text{bulk}}} = \left( \frac{M_i}{M_j} \right)^2$$

On the other hand, the ratio  $M_{i,z}/M_{j,z}$  for the bands at a LB film is equal to the ratio  $I_i^{\text{LB}}/I_j^{\text{LB}}$ . Thus, the tilt angle  $\Theta$  of the transition moment  $M_i$  can be evaluated using following equation:

$$\text{tg}^2 \theta = \frac{I_i^{\text{bulk}} I_j^{\text{LB}}}{I_j^{\text{bulk}} I_i^{\text{LB}}}$$

This relative method was described in details by Debe [276] and Arnold et al. [277] and several times was used successfully by the authors of this review article [272,279–281].

Porphyrins and similar to them phthalocyanines are organic chromophores commonly used in various photovoltaic applications. To learn more about the effect of chemical properties and spatial conformation of various phthalocyanine substituents leading to extension of their  $\pi$ -electron system, we systematically investigated the spectroscopic response of bulk and thin film samples of a large family of copper phthalocyanines [281]. The reflection–absorption spectra of the samples with the use of the unpolarised and polarised light, with electric vector of the light wave parallel ( $0^\circ$ ;  $p$ -polarisation) or perpendicular ( $90^\circ$ ;  $s$ -polarisation) to the plane of incidence were recorded



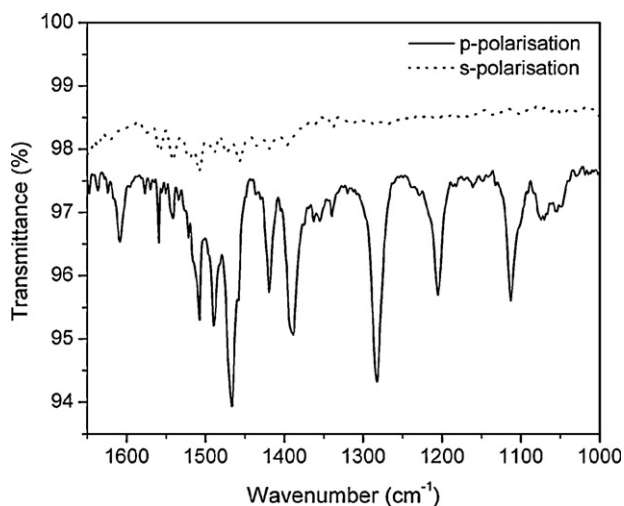


**Fig. 4.14.** IRRA spectrum of copper(II) 2,3,9,10,16,17,23,24-octakis(octyloxy)-29H,31H-phthalocyanine for two perpendicular light polarisations.

in the range 400–4000  $\text{cm}^{-1}$ . For spectroscopic investigation we have chosen the films of five or ten layers. In our evaluations we applied the simplified method proposed by Arnold et al. [277]. The typical IRRA spectra of copper(II) 2,3,9,10,16,17,23,24-octakis(octyloxy)-29H,31H-phthalocyanine, for two perpendicular light polarisations, restricted to the most informative region from 1000 to 1800  $\text{cm}^{-1}$  are shown in Fig. 4.14. For estimation of the molecular orientation of the macrocyclic central part of phthalocyanines and substituent groups, about ten most intensive and relatively well resolved reflection–absorption bands have been selected. There are two main conclusions from these investigations: (i) the tilt angle  $\Theta$  for the transition moment of the bands which are connected with bending or deformations of the macro-cycle is  $(45 \pm 3)^\circ$ , (ii) the value of the estimated tilt angle  $\Theta$  for a few bands attributed to vibrations of the substituent is  $(55 \pm 3)^\circ$ . This means that the macroring of the phthalocyanine is tilted to the normal by about  $45^\circ$  but the substituent is inclined from the plane of the cycle by about  $10^\circ$  [282].

Electronic absorption and IRRA spectra of lead porphyrin as well as magnesium and lead phthalocyanine dyes deposited in the form of LB nanolayers on various solid inorganic surfaces were discussed in the paper of Lewandowska et al. [279]. The IR spectroscopy was supported by UV–vis absorption studies to follow the interaction at the interface between the dye layers and the substrates as well as to evaluate linear dichroism and to determine the arrangement of molecules in the LB films. Analysis of the film dichroism indicated that the phthalocyanine molecular frame is oriented at about  $45^\circ$  with respect to  $x$ - and  $y$ -axes ( $x$ - and  $y$ -axes lie in the plane of the solid substrate).

Dyads of the type fullerene–organic chromophore are particularly interesting from the application point of view. Materials of this type investigated recently by us are the dyads PDI– $\text{C}_{60}$  and PDI–TTF [280]. Comparison of the absorption and IRRA spectra of the multilayered LB samples of these dyads suggests small redistribution of charges in both moieties of the dyads after LB layer formation. Otherwise, charge redistribution is especially distinct for the bands assigned to external part of the PDI molecules suggesting, that the dyads are fastened to the gold substrate surface with the PDI end. The orientation of the organic chain molecules grafted to the gold surface was evaluated by comparing IRRA and IR absorption data. Polarised IRRA spectra for 10 layers of LB film of the PDI– $\text{C}_{60}$  dyad on Au substrate are shown in Fig. 4.15. It was found that the PDI moiety is tilted to the normal by about  $44^\circ$  in the PDI– $\text{C}_{60}$  dyad, and by about  $52^\circ$  in PDI–TTF one. The linked parts of the dyads are slightly inclined to the plane of the PDI molecule [280].

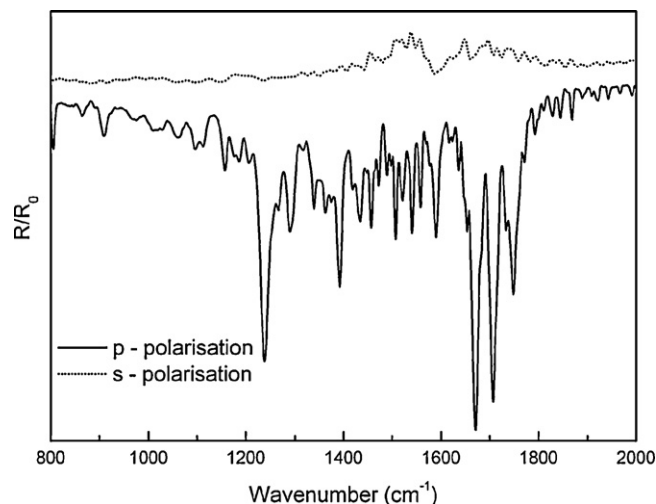


**Fig. 4.15.** Polarised IRRA spectra for 10 layers of LB film of PDI– $\text{C}_{60}$ .

Langmuir–Blodgett films of the dyads of fullerene and porphyrin-derived dyes of different thicknesses were studied at various angles of light beam incidence and two mutually perpendicular  $p$ - and  $s$ -light polarisations by both IRRA and UV–vis methods [14]. These methods provided information on layer organisation, in particular on the molecule orientation. For example, the polarised UV–vis spectra of P– $\text{C}_{60}$  dyad are shown in Fig. 4.16. The parameter  $P_x$ , corresponding to the fraction of molecules with centre axis  $z'$  projections parallel to the Cartesian  $x$  axis, proposed by Yoneyama et al. [289] gives information on the orientation of the molecular plane to the  $x$  axis. The data needed for the parameter determination are accessible from the polarised spectra of the dyes and fullerene–dye dyads shown in Fig. 4.16 and similar spectra for the other porphyrin–fullerene dyads discussed in [281].

The polarised UV–vis spectra of the LB layers of porphyrin P and its dyad 2P are nearly identical for both  $p$ - and  $s$ -polarisations of light (not shown) and the  $P_x$  value for the dyes is of about 0.47. The  $P_x$  value less than 0.5 suggests insignificant ordering of the molecular planes to the  $y$  axis. Similarly, insignificant changes in the orientation of porphyrin cycle in the dyad P– $\text{C}_{60}$  was concluded taking into account the value of the parameter  $P_x$  approximating 0.5. The situation is different from that for the dyads 2P– $\text{C}_{60}$  and 2P–2 $\text{C}_{60}$ . The angle  $\theta$  evaluated from the value of  $\langle \cos^2 \theta \rangle$  and  $P_x$  of

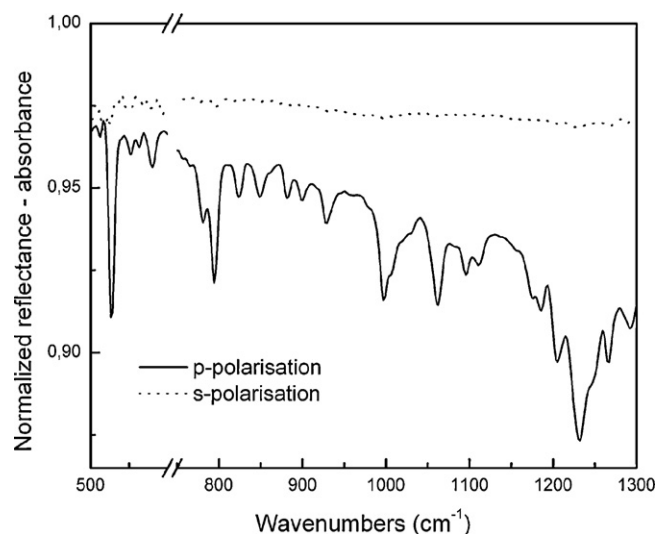


**Fig. 4.16.** Polarised UV–vis spectra of the LB layers of P– $\text{C}_{60}$  dyad.

the Soret band is between 33 and 55° but of the Q band – between 55 and 65°. These data show that bonding of the porphyrin dimer to fullerene leads to a certain reorientation of the porphyrin moieties. On the other hand, there is a difference in the  $\theta$  angle evaluated from various absorption bands. This effect could of course arise from different configurations of the molecular orbitals taking part in both discussed electron transitions for which the transition moment directions are different. In conclusion, it seems that distinct reorientation of the porphyrin-derived moieties bonded to fullerene could be induced by some changes in the chromophore symmetry induced by the presence of a large, spherical C<sub>60</sub> molecule.

## 5. Towards prospective applications

A number of prospective applications of the donor–acceptor systems have been proposed. Among them are such fascinating applications as various photonic devices, light emitting diodes, field-effect transistors and organic memories for molecular computers, logic gates, sensors, switches, and catalysts [5–7,209,290,291]. In principle, devices using organic materials should be cheaper and simpler to manufacture than the corresponding ones produced from inorganic materials. Maybe for this reason, organic devices converting solar energy into electrical one are in the centre of interest at the majority of laboratories working in the field of molecular engineering [125,292–294]. That is why, in this chapter, we concentrated on the solar energy conversion devices based on the energy and/or electron transfer between organic chromophores and suitable electron acceptors. On the other hand, the fundamental processes occurring in photovoltaic systems are the main subject of our investigation, partially summarized in this review article.

Organic solar cell research and development of related devices have still a long way to go to compete with inorganic solar cells. The efficiency of inorganic solar cells goes up to 20% but organic solar cells operate usually at the efficiency of 5–6% [293]. An exception is ruthenium polypyridyl complex as TiO<sub>2</sub> sensitizer with N3 dye demonstrating photovoltaic cell energy conversion efficiency of 11% [295]. There are several physical reasons for the low efficiency of organic systems [292]. One of them is the generally poor charge-carrier mobility of organic solids, a few orders of magnitudes lower than that in inorganic ones [296]. This effect is partly balanced by relatively strong absorption coefficients, usually  $\geq 10^5 \text{ cm}^{-1}$  [294]. Another important difference between crystalline inorganic materials and rather amorphous and disordered organic materials is the relatively small diffusion length of primary photoexcitations [294–299]. These features of organic systems lead to devices with very small layer thickness, very often below 100 nm. Typical and simplest construction of organic solar cell is shown in Fig. 5.1.

Molecular and polymer photovoltaics are distinguished by the type of materials and production methods. Molecular photovoltaic devices are generally made by sublimation of successive layers of electron- and hole-transporting materials. Charge photogeneration occurs at the interface between two layers (organic heterojunction). The first organic solar cell exhibiting reasonable power conversion efficiencies (nearly 1%), using phthalocyanine and perylene derivatives, was obtained by Tang [300]. Now, the fullerene and its derivatives [291] are widely investigated with the aim of designing solar energy converters, both as separate layers in molecular organic photovoltaic devices and in bulk heterojunction polymer organic photovoltaic cells.

One of the primary limitations of a heterojunction solar cell is that charge photogeneration takes place only in a thin layer near the heterojunction. One way to increase the width of the photocarrier generation region is to co-evaporate two organic dyes to create a bulk heterojunction. Improvements in device per-

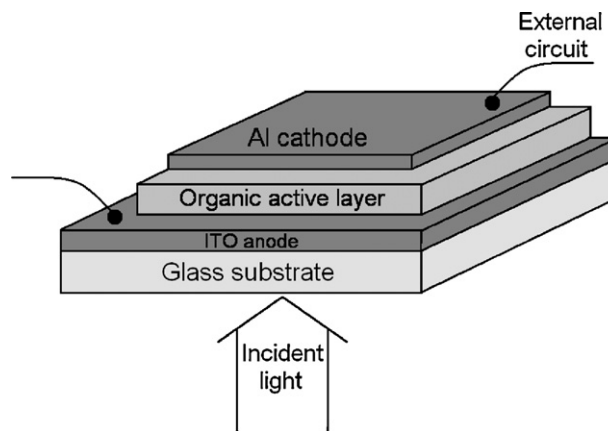


Fig. 5.1. Typical construction of an organic solar cell.

formance were obtained by co-deposited layer containing equal weights of C<sub>60</sub> and chromophore as charge photogeneration layer in organic photovoltaic devices based on perylene, porphyrin and phthalocyanine derivatives; the efficiency of power conversion for this cell was 1.05% [301]. Power conversion efficiencies of 3.37% under 10 mW/cm<sup>2</sup> and 1.04% under 100 mW/cm<sup>2</sup> white light were reported by Gebeyehu et al. [302] for a similar structure with some amine as a hole-transporting layer. It was shown that the power efficiency of molecular organic photovoltaic cells could be limited by the morphology of the bulk heterojunction [303]. Five years ago the Princeton group reported a molecular organic photovoltaic device with the power conversion efficiency of 4.2%; the device structure was ITO/CuPc/C<sub>60</sub>/blocking layer/Ag [304]. The power conversion efficiency increased with increasing incident power density, reaching a maximum conversion of 4.2% under 4–12 suns simulated illumination. The high efficiency of this photovoltaic cell was attributed to a very low series resistance of  $\sim 0.1 \Omega/\text{cm}^2$ , resulting in devices with fill factors as high as 0.6 [304].

The power conversion efficiency and photovoltage can be broken through by making tandem solar cells. This type of solar cell consists of several stacked solar cells made from materials with different optical gaps. Sunlight is first absorbed by the higher-gap cell. Lower energy photons pass through the higher gap device and are absorbed by the second cell [305].

Recent information on progress in understanding of molecular solar cells, development of novel conjugated donor dyes for high-efficiency bulk heterojunction photovoltaic devices, strategies for increasing the efficiency of heterojunction organic solar cells, material for solar cells selection, device architecture, critical interfaces and their influence on the open-circuit voltage, recent advances in sensitised mesoscopic solar cells, recombination in quantum dot sensitised solar cells and other interesting data, can be found in the special issue of the Account of Chemical Research entitled Organic Photovoltaics [306].

## Acknowledgements

The research reported was supported by the Ministry of Science and Higher Education, Poland within the research project to be realised in the years 2008–2011. The authors are much grateful to Prof. Diederich and Dr. Bonifazi (Zürich, Switzerland) and Prof. Imahori (Kyoto, Japan) for the gifts of the porphyrin-derived samples, Prof. Hudhomme (Angers, France) for preparation PDI-derived dyads, and Prof. K.-S. Lee (Daejeon, South Korea) for presenting us with the fullerene–thiophene-based dyads. Our deep thanks go to our co-workers Drs B. Barszcz, A. Biadasz, K. Lewandowska, and A. Łapiński for stimulating discussions and kind assistance. The

authors are particularly grateful to M.Sc. A. Bogucki for preparation of the figures.

## References

- [1] C.C. Moser, J.M. Keske, K. Warncke, R.S. Farid, P.L. Dutton, *Nature* 355 (1992) 796.
- [2] N.W. Woodbury, J.P. Allen, in: R.E. Blankenship, M.T. Madigan, C.E. Bauer (Eds.), *Anoxygenic Photosynthetic Bacteria*, Kluwer Academic Publishers, Dordrecht, 1995, p. 527.
- [3] S. Mattes, S. Farid, *Science* 226 (1984) 917.
- [4] D. Gust, T.A. Moore, A.L. Moore, in: Z.W. Tian, Y. Cao (Eds.), *Photochemical and Photoelectrochemical Conversion and Storage of Solar Energy*, International Academic Publishers, Beijing, 1993.
- [5] H. Imahori, Y. Mori, Y. Matano, *J. Photochem. Photobiol. C: Photochem. Rev.* 4 (2003) 51.
- [6] H. Imahori, *Org. Biomol. Chem.* 2 (2004) 1425.
- [7] D.M. Guldi, *Chem. Soc. Rev.* 31 (2002) 22.
- [8] R.A. Marcus, *Annu. Rev. Phys. Chem.* 15 (1964) 155.
- [9] R.A. Marcus, *Angew. Chem., Int. Ed. Engl.* 32 (1993) 1111.
- [10] P.A. Lane, Z.H. Kafafi, in: S.-S. Sun, N.S. Sariciftci (Eds.), *Organic Photovoltaics. Mechanisms, Materials, and Devices*, CRC Press, Taylor & Francis Group, 2005, p. 49.
- [11] M.E. El-Khouly, O. Ito, P.M. Smith, F. D'Souza, J. Photochem. Photobiol. C: Photochem. Rev. 5 (2004) 79.
- [12] J.S. Connolly, J.R. Bolton, in: M.A. Fox, M. Chanon (Eds.), *Photoinduced Electron Transfer*, Elsevier, Amsterdam, 1988, p. 303.
- [13] V. Balzani, *Electron Transfer in Chemistry*, vols. I–V, Wiley-VCH, Weinheim, 2001.
- [14] J.W. Verhoeven, L.P. Dirkxm, T.J. Deboer, *Tetrahedron Lett.* 7 (1966) 4399.
- [15] D.I. Schuster, P. Cheng, P.D. Jarowski, D.M. Guldi, C. Luo, L. Echegoyen, S. Pyo, A.R. Holzwarth, S.E. Braslavsky, R.M. Williams, G. Klich, *J. Am. Chem. Soc.* 126 (2004) 7257.
- [16] Ch.S. Foote, *Topics in Current Chemistry. Photophysical and Photochemical Properties of Fullerene*, vol. 169, Springer-Verlag, Berlin/Heidelberg, 1994, p. 349.
- [17] D. Bonifazi, F. Diederich, *Chem. Commun.* (2002) 2178.
- [18] M.S. Dresselhaus, G. Dresselhaus, P.C. Eklund, *Science of Fullerenes and Carbon Nanotubes*, Academic Press, San Diego/Boston/New York/London/Sydney/Tokyo/Toronto, 1996.
- [19] F. Diederich, M. Gómez-López, *Chem. Soc. Rev.* 28 (1999) 263.
- [20] H. Scheer (Ed.), *Chlorophylls*, CRC Press, Boca Raton/Ann Arbor/Boston/London, 1991.
- [21] J.C. Martins, L.A. Sousa, *Bioelectronic Vision: Retina Models, Evaluation Matrices and System Design*, World Scientific Publ. Co. Pte Ltd, 2009.
- [22] L. Sherwood, in: P. Adams, N. Rose (Eds.), *Fundamentals of Physiology. A Human Perspective*, Thomson Brooks/Cole, USA, 2006.
- [23] M. Kaneko, I. Okura (Eds.), *Photocatalysis. Science and Technology*, Kodansha Ltd. Tokyo, Springer-Verlag, Berlin/Heidelberg/New York, 2002.
- [24] J.D. Regan, J.A. Parrish (Eds.), *The Science of Photomedicine*, Plenum, New York/London, 1982.
- [25] C. Brabec, V. Dyakonov, U. Scherf (Eds.), *Organic Photovoltaics: Materials, Devices, Physics, Manufacturing, Technologies*, Wiley-VCH, Verlag GmbH & Co. KGaA, Weinheim, 2008.
- [26] H. Klauk (Ed.), *Organic Electronics: Materials, Manufacturing and Application*, Wiley-VCH, Verlag GmbH & Co. KGaA, Weinheim, 2006.
- [27] C.M. Drain, A. Varroto, I. Radivojevic, *Chem. Rev.* 109 (2009) 1630.
- [28] Th. Förster, *Z. Natur.* 4a (1949) 321.
- [29] J.B. Birks, S. Georgiou, *J. Phys. B1* (1968) 958.
- [30] A.G. Tweed, W.D. Bellamy, G.L. Gaines, *J. Chem. Phys.* 41 (1964) 2068.
- [31] I.Z.S. Steinberg, *J. Chem. Phys.* 48 (1968) 2411.
- [32] R.M. Pearlstein, in: Govindjee (Ed.), *Photosynthesis, Energy Conversion by Plants and Bacteria*, vol. 1, Academic Press, New York, 1982, p. 293.
- [33] A. Laganà, G. Lendvay (Eds.), *Theory of Chemical Reaction Dynamics*, NATO Sciences Service, Kluwer Academic Publishers, Dordrecht, 2004.
- [34] V. May, O. Kühn, *Charge and Energy Transfer in Molecular Systems*, Wiley-VCH, Verlag GmbH & Co. KGaA, Weinheim, 2004.
- [35] Th. Förster, in: O. Sinanoghi (Ed.), *Modern Quantum Chemistry. Delocalized excitation and excitation Transfer*, Academic Press, New York, 1965, pp. 93–137.
- [36] D.L. Dexter, *J. Chem. Phys.* 21 (1953) 836.
- [37] R.A. Marcus, *J. Chem. Phys.* 24 (1956) 966.
- [38] R.A. Marcus, *J. Chem. Phys.* 43 (1965) 679.
- [39] R.A. Marcus, *J. Phys. Chem.* 72 (1968) 891.
- [40] R.A. Marcus, N. Sutin, *Biochim. Biophys. Acta* 811 (1985) 265.
- [41] S.F. Nelsen, J. Adamus, J.J. Wolff, *J. Am. Chem. Soc.* 116 (1994) 1589.
- [42] K. Yates, *J. Phys. Org. Chem.* 2 (1988) 300.
- [43] D.N. Silverman, *Biochim. Biophys. Acta: Bioenergetics* 1458 (2000) 88.
- [44] R.H. Hill, *J. Chem. Soc.: Chem. Commun.* (1989) 293.
- [45] R.M. Lynden-Bell, *Electrochem. Commun.* 9 (2007) 1857.
- [46] H. Tributsch, L. Pohlmann, *Science* 279 (1998) 1891.
- [47] M. Mehanna, R. Basseguya, M.-L. Deliaa, Alain Bergela, *Electrochem. Commun.* 11 (2009) 568.
- [48] A.Y. Musa, A.A.H. Kadhum, A.B. Mohamad, A.A.B. Rahoma, H. Mesmari, *J. Mol. Struct.* 969 (2010) 233.
- [49] M.A. Hough, M.J. Ellis, S. Antonyuk, R.W. Strange, G. Sawers, R.R. Eady, S.S. Hasnain, *J. Mol. Biol.* 350 (2005) 300.
- [50] J.B. Birks, *Photophysics of Aromatic Molecules*, Wiley-Interscience Public, London/New York, 1973.
- [51] J. Lakowicz, *Principle of Fluorescence Spectroscopy*, Plenum Press, New York, 1999.
- [52] S. Murata, S.Y. Matsuzaki, M. Tachiya, *J. Phys. Chem.* 99 (1995) 5354.
- [53] J.A. Weil, J.R. Bolton (Eds.), *Electron Spin Resonance. Elementary Theory and Practical Applications*, Wiley Interscience/J. Wiley and Sons Inc., Hoboken, NJ, 2007.
- [54] M. Godlewski, *Appl. Mag. Res.* 2 (1991) 349.
- [55] S.E. Braslavsky, K. Heihoff, in: J.C. Scaiano (Ed.), *CRC Handbook of Organic Photochemistry*, vol. 1, CRC Press, Boca Raton, FL, 1989, p. 327.
- [56] S.E. Braslavsky, G.E. Heibel, *Chem. Rev.* 92 (1992) 1381.
- [57] A. Rosencwaig, *Photoacoustics and Photoacoustic Spectroscopy*, Wiley-Interscience, New York, 1980.
- [58] D. Cahen, H. Garty, R.S. Becker, *J. Phys. Chem.* 84 (1980) 3384.
- [59] E.P. Tomasini, E. San Roman, S.E. Braslavsky, *Langmuir* 25 (2009) 5861.
- [60] S.E. Braslavsky, *Photochem. Photobiol.* 43 (1986) 667.
- [61] C. Serpa, J. Schabauer, A.P. Piedade, C.J.P. Monteiro, M.M. Pereira, P. Douglas, H.D. Burrows, L.G. Arnaut, *J. Am. Chem. Soc.* 130 (2008) 8876.
- [62] T.A. More, D. Benin, R. Tom, *J. Am. Chem. Soc.* 104 (1982) 7356.
- [63] M. Ouzafe, P. Poulet, J. Chabron, *J. Photochem. Photobiol. A: Chem.* 181 (2006) 491.
- [64] K. Gibasiewicz, R. Naskręcki, M. Ziółek, M. Lorenc, J. Karolczak, J. Kubicki, J. Goc, J. Miyake, A. Dobek, *J. Fluorescence* 11 (2001) 33.
- [65] W. Gruszecki, R. Luchowski, M. Zubik, W. Grudziński, E. Janik, M. Gospodarek, J. Goc, Z. Gryczyński, I. Gryczyński, *J. Plant Physiol.* 167 (2010) 69.
- [66] A. Siejak, D. Wróbel, R.M. Ion, *J. Photochem. Photobiol. A: Chem.* 181 (2006) 180.
- [67] B. Olejarz, B. Bursa, I. Szyperska, R.M. Ion, A. Dudkowiak, *Int. J. Thermophys.* 31 (2010) 163.
- [68] N.A. Borisevich, G.A. Zaleskaya, A.E. Urbanovich, *Spectr. Lett.* 23 (1990) 405.
- [69] D. Wróbel, J. Łukasiewicz, H. Manikowski, *Dyes Pigments* 58 (2003) 7.
- [70] M. Migita, T. Okada, N. Mataga, S. Nishitani, N. Kurata, Y. Sakata, S. Misami, *Chem. Phys. Lett.* 84 (1981) 263.
- [71] S. Nishitani, N. Kurata, Y. Sakata, S. Misami, A. Karen, T. Okada, N. Mataga, *J. Am. Chem. Soc.* 105 (1983) 7771.
- [72] H. Imahori, K. Hagiwara, T. Akiyama, M. Aoki, S. Taniguchi, T. Okada, M. Shirakawa, Y. Sakata, *Chem. Phys. Lett.* 263 (1996) 545.
- [73] D. Gust, T.A. Moore, A.L. Moore, *J. Photochem. Photobiol. B* 58 (2000) 63.
- [74] H. Imahori, Y. Kashiagi, T. Hasobe, M. Kimura, T. Hanada, Y. Nishimura, I. Yamazaki, Y. Araki, O. Ito, S. Fukuzumi, *Thin Solid Films* 451–452 (2004) 580.
- [75] S. Sariciftci, F. Wudl, A.J. Heeger, M. Maggini, G. Scarrano, M. Prato, J. Bourassa, P.C. Ford, *Chem. Phys. Lett.* 247 (1995) 510.
- [76] A.L. Moore, T.A. Moore, D. Gust, J.J. Silber, L. Sereno, F. Fungo, L. Otero, G. Steinberg-Yfrach, P.A. Liddell, S.C. Hung, H. Imahori, S. Carsodo, D. Tatman, A.N. Macpherson, *Pure Appl. Chem.* 69 (1997) 2111.
- [77] N.V. Tkachenko, V. Vehmanen, J.P. Nikkanen, H. Yamada, H. Imahori, S. Fukuzumi, H. Lemmentyinen, *Chem. Phys. Lett.* 366 (2002) 245.
- [78] D.M. Guldi, M. Prato, *Acc. Chem. Res.* 33 (2000) 695.
- [79] T. Kato, M. Tachiya, *Chem. Phys. Lett.* 241 (1995) 463.
- [80] P. Hudhomme, C. Boule, J.M. Rabreau, M. Cariou, M. Jubault, A. Gorgues, *Synth. Metals* 94 (1998) 73.
- [81] J. Fortage, J. Boixel, E. Blart, L. Hammarström, H.C. Becker, F. Odobel, *Chemistry* 14 (2008) 3467.
- [82] H. Imahori, K. Tamaki, H. Yamada, K. Yamada, Y. Sakata, Y. Nishimura, I. Yamazaki, M. Fujitsuka, O. Ito, *Carbon* 38 (2000) 1599.
- [83] D.M. Guldi, K.D. Asmus, *J. Am. Chem. Soc.* 119 (1997) 5744.
- [84] D.M. Guldi, C. Luo, A. Swartz, M. Scheloske, A. Hirsch, *Chem. Commun.* (2001) 1066.
- [85] A.S. Davydov, *Theory of Molecular Excitons*, McGraw-Hill, New York, 1962.
- [86] M. Kasha, H.R. Rawls, M.A. El-Bayoumi, *Pure Appl. Chem.* 11 (1965) 371.
- [87] W. Brütting (Ed.), *Physics of Organic Semiconductors*, Wiley-VCH Verlag, GMBH Co. KGaA, Weinheim, 2005.
- [88] I. Beletskaya, V.S. Yurina, A.Y. Tsvadze, R. Guillard, C. Stern, *Chem. Rev.* 109 (2009) 1659.
- [89] Govindjee, *Photosynthesis. Energy Conversion*, Academic Press, New York, 1982.
- [90] A. Facchetti, *Mater. Today* 10 (2007) 28.
- [91] H. Kautsky, H. Berkel, *Naturwissenschaften* 27 (1939) 195.
- [92] G.L. Levison, W.T. Simpson, W. Curtis, *J. Am. Chem. Soc.* 79 (1957) 4314.
- [93] A. Szent-Györgyi, *Sciences* 124 (1956) 873.
- [94] Th. Förster, *Naturwissenschaften* 36 (1949) 240.
- [95] A.J. Hoff, J. Ames, in: H. Scheer (Ed.), *Chlorophylls*, CRC Press, Boca Raton/Ann Arbor/Boston/London, 1991, p. 723.
- [96] W. Fudickar, J. Zimmermann, L. Ruhlmann, J. Schneider, B. Röder, U. Siggel, J.-H. Fuhrhop, *J. Am. Chem. Soc.* 121 (1999) 9539.
- [97] R. Pottier, A. Lachaine, M. Pierre, J.C. Kennedy, *Photochem. Photobiol.* 47 (1988) 669.
- [98] E. Orti, J.L. Bredas, C.J. Clarisse, *Chem. Phys.* 92 (1990) 1228.
- [99] N.C. Maiti, S. Mazumdar, N. Reriasamy, *J. Phys. Chem.* 102 (1998) 1528.
- [100] E.S. Dodsworth, A.B.P. Lever, P. Seymour, C.C. Leznoff, *J. Phys. Chem.* 89 (1985) 5698.
- [101] Z. Gasyna, N. Kobayashi, M.J. Stillman, *J. Chem. Soc. Dalton Trans.* 14 (1989) 2397.

- [102] A.J. Barnes, Proceedings of the 8th International Conference on Molecular Spectroscopy, Wrocław-Lądek Zdrój, 2005, p. 09.
- [103] M. Ogawa, N. Kosaka, P.L. Choyke, H. Kobayashi, *ACS Chem. Biol.* 17 (2009) 535.
- [104] M.K. Johansson, H. Fidder, D. Dick, R.M. Cook, *J. Am. Chem. Soc.* 124 (2002) 6950.
- [105] F. del Monte, D. Levy, *J. Phys. Chem. B* 102 (1998) 8036.
- [106] A. Boguta, A. Wójcik, R.M. Ion, D. Wróbel, *J. Photochem. Photobiol. A: Chem.* 163 (2004) 201.
- [107] K. Kameyama, M. Morisue, A. Satake, Y. Kobuke, *Angew. Chem.* 117 (2005) 4841.
- [108] D. Wróbel, A. Boguta, A. Wójcik, R.M. Ion, *Nonlinear Opt. Quantum Opt.* 31 (2004) 333.
- [109] A. Siejak, D. Wróbel, Yu.S. Avlasevich, *J. Phys. IV France* 137 (2006) 331.
- [110] A. Siejak, D. Wróbel, B. Laskowska, Yu.S. Avlasevich, *Spectrochim. Acta Part A: Mol. Biomol. Spectr.* 74 (2009) 148.
- [111] J.B. Birks, *Rep. Prog. Phys.* 38 (1975) 903.
- [112] D. Basting, G. Marowski (Eds.), *Excimer Laser Technology*, Springer, Berlin, 2004.
- [113] D. Sahoo, V. Narayanaswami, C.M. Kay, R.O. Ryan, *Biochemistry* 39 (2000) 6594.
- [114] T. Sagawa, S. Fukugawa, T. Yamada, H. Ihara, *Langmuir* 18 (2002) 7223.
- [115] E. Kostenko, M. Dobrikov, D. Pyshnyi, V. Petyuk, N. Komarova, V. Vlassov, M. Zenkova, *Nucl. Acids Res.* 29 (2001) 3611.
- [116] T. Ikka, T. Arai, K. Shimada, *J. Fluorescence* 16 (2006) 367.
- [117] D. Wróbel, A. Graja, *J. Photochem. Photobiol. A: Chem.* 183 (2006) 79.
- [118] A.M. Kuznetsov, *Charge Transfer in Physics, Chemistry and Biology. Physical Mechanism of Elementary Processes and An Introduction to The Theory*, OPA – Gordon and Breach Publ., Amsterdam, 1995.
- [119] S.A. Odom, M.M. Caruso, A.D. Finke, A.M. Prokup, J.A. Ritchey, J.H. Leonard, S.R. White, N.R. Sottos, J.S. Moore, *Adv. Functional Mater.* (2010), doi:10.1002/adfm.201000159.
- [120] K.M. Jain, A. Hundet, P. Pal, T.N. Misra, *J. Mater. Sci. Lett.* 10 (1991) 71.
- [121] M. Zheng, V.V. Rostovtsev, *J. Am. Chem. Soc.* 128 (2006) 7702.
- [122] D. Holten, D.F. Bocian, J.S. Lindsey, *Acc. Chem. Res.* 35 (2002) 57.
- [123] Y. Vida, R. Suau, J. Casado, A. Berlin, J.T. López Navarrete, E. Pérez-Inestrosa, *Macromol. Rapid Commun.* 28 (2007) 1345.
- [124] S.Y. Kim, K.H. Lee, B.D. Chin, J.-W. Yu, *Sol. Energy Mater. Sol. Cells* 93 (2009) 129.
- [125] S.-S. Sun, N.S. Sariciftci (Eds.), *Organic Photovoltaics. Mechanisms, Materials, and Devices*, CRC Press/Taylor & Francis Group, 2005.
- [126] S. Leach, M. Vervloet, A. Després, E. Bréheret, J.P. Hare, T.J. Dennis, H.W. Kroto, R. Taylor, D.R.M. Walton, *Chem. Phys.* 160 (1992) 451.
- [127] Y. Zeng, L. Biczok, H. Linschitz, *J. Phys. Chem.* 96 (1992) 5237.
- [128] A.L. Balch, V.J. Catalano, J.W. Lee, *Inorg. Chem.* 30 (1991) 3980.
- [129] O. Diels, K. Alder, *Justus Liebig's Annalen Chemie* 460 (1928) 98.
- [130] P.A. Troshin, R.N. Lyubovskaya, *Russian Chem. Rev.* 77 (2008) 305.
- [131] M. Gouterman, in: D. Dolphin (Ed.), *The Porphyrins*, vol. 3, Academic Press, New York, 1978, p. 1.
- [132] M. Gouterman, *J. Chem. Phys.* 30 (1959) 1139.
- [133] J. Zimmermann, U. Siggel, J.-H. Fuhrhop, B. Röder, *J. Phys. Chem. B* 107 (2003) 6019.
- [134] D. Dolphin, *The Porphyrins*, vol. III, Academic Press, 1978.
- [135] C.C. Leznoff, A.P.B. Lever (Eds.), *Phthalocyanines – Properties and Applications*, Wiley-VCH, New York, Weinheim, 1989.
- [136] H. Du, R.A. Fuh, J. Li, A. Corman, J.S. Lindsey, *Photochem. Photobiol.* 68 (1998) 141.
- [137] I.B. Berlman, *Handbook of Fluorescence Spectra of Aromatic Molecules*, Academic Press, New York, 1965.
- [138] H. Içil, E. Arslan, *Spectr. Lett.* 34 (2001) 355.
- [139] Y. Shibano, T. Ureyama, Y. Matano, N.V. Tkachenko, H. Lemmetyinen, H. Imahori, *Org. Lett.* 8 (2006) 4425.
- [140] C. Karapire, C. Zafer, S. İçli, *Synth. Met.* 145 (2004) 51.
- [141] A. Łapiński, A. Graja, I. Olejniczak, A. Bogucki, M. Połomska, J. Baffreau, L. Perkin, S. Leroy-Lhez, P. Hudhomme, *Mol. Cryst. Liq. Cryst.* 447 (2006), 87/[405]–103/[421].
- [142] J. Swanson, *Ullmann's Encyclopedia of Industrial Chemistry*, Wiley-VCH, Weinheim, 2006.
- [143] J.M. Tour, *Chem. Rev.* 96 (1996) 537.
- [144] R.E. Martin, F. Diederich, *Angew. Chem. Int. Ed.* 38 (1999) 1350.
- [145] B. O'Regan, M. Grätzel, *Nature* 353 (1991) 737.
- [146] J. Bisquert, D. Cahen, G. Hodes, S. Rühle, A. Zaban, *J. Phys. Chem. B* 108 (2004) 8106.
- [147] K. Kalyanasundaram, M. Grätzel, *Coord. Chem. Rev.* 77 (1998) 347.
- [148] T. Gerfin, M. Grätzel, L. Walder, *Prog. Inorg. Chem.* 44 (1997) 345.
- [149] A. Hagfeldt, M. Grätzel, *Chem. Rev.* 95 (1995) 49.
- [150] N. Rossier-Iten, *Solid hybrid dye-sensitized solar cells: new organic materials, charge recombination and stability*, Ph.D. Thesis, EPFL, Lausanne, 2006.
- [151] Q. Wang, W. Campbell, E. Bonfantani, K. Jolley, D. Officer, P. Walsh, K. Gordon, R. Humphry-Baker, M. Nazeeruddin, M. Grätzel, *J. Phys. Chem. B* 109 (2005) 15397.
- [152] B. Yu, *Nat. Mater.* 7 (2008) 626.
- [153] M. Grätzel, *Inorg. Chem.* 44 (2005) 6841.
- [154] A. Morandeira, I. López-Duarte, M.V. Martínez-Díaz, B. O'Regan, C. Shuttle, N.A. Haji-Zainulabidin, T. Torres, E. Palomares, J.R. Durrant, *J. Am. Chem. Soc.* 129 (2007) 9250.
- [155] L. Luo, C.J. Lin, C.Y. Tsai, H.P. Wu, L.L. Li, C.F. Lo, C.Y. Lin, E.W. Diau, *Phys. Chem. Chem. Phys.* 7 (2010) 1064.
- [156] T.A. Heimer, E.J. Heilweil, *J. Phys. Chem.* 101 (1997) 10990.
- [157] T. Hasobe, H. Imahori, P.V. Kamat, T.K. Ahn, S.K. Kim, D. Kim, A. Fujimoto, T. Hirakawa, S. Fukuzumi, *J. Am. Chem. Soc.* 127 (2005) 1216.
- [158] L. Schmidt-Mende, W.M. Campbell, Q. Wang, K.W. Jolley, D.L. Officer, M.K. Nazeeruddin, M. Grätzel, *Chem. Phys.* 6 (2005) 1253.
- [159] M.W. Lee, D.L. Lee, W.N. Yen, C.Y. Yeh, *J. Macromol. Sci. Part A* 46 (2009) 730.
- [160] P.S. Smertenkova, V.P. Kostyleva, V.V. Kislyukb, A.F. Syngaevskaya, S.A. Zynioa, O.P. Dimitrieva, *Sol. Energy Mater. Sol. Cells* 92 (2008) 976.
- [161] D. Wróbel, J. Goc, R.M. Ion, *J. Mol. Struct.* 450 (1998) 239.
- [162] D. Wróbel, A. Siejak, P. Siejak, *Sol. Energy Mater. Sol. Cells* 94 (2010) 492.
- [163] A. Siejak, D. Wróbel, B. Olejars, R.M. Ion, *Dyes Pigments* 83 (2009) 281.
- [164] D. Wróbel, A. Boguta, in: A. Graja, B. Bułka, F. Kajzar (Eds.), *Molecular Low Dimensional and Nanostructured Materials for Advanced Applications*, Kluwer Academic Publishers, The Netherlands, 2002, p. 71.
- [165] D. Wróbel, J. Łukasiewicz, J. Goc, A. Waszkowiak, R.M. Ion, *J. Mol. Struct.* 555 (2000) 407.
- [166] D. Wróbel, A. Boguta, *J. Photochem. Photobiol. A: Chem.* 150 (2002) 67.
- [167] N. Wakao, N. Yokoi, N. Isayama, A. Hirashi, K. Shimana, M. Kobayashi, H. Kise, M. Iwaki, S. Itoh, S. Takaichi, Y. Sakuri, *Plant Cell Physiol.* 37 (1996) 127.
- [168] H.C. Lukaski, *Am. Soc. Clin. Nutr.* 72 (2000) 585SS.
- [169] D. Wróbel, C. R. Chim. 6 (2003) 417.
- [170] M. Gouterman, L. Stryer, *J. Chem. Phys.* 37 (1962) 2260.
- [171] J. Chen, D.L. Officer, J.M. Pringle, D.R. MacFarlane, C.O. Too, G.G. Wallace, *Electrochem. Solid-State Lett.* 8 (2005) A528–A530.
- [172] J. Chen, A.K. Burrell, W.M. Campbell, D.L. Officer, C.O. Too, G.G. Wallace, *Electrochim. Acta* 49 (2004) 329.
- [173] K. Sugawa, K. Kakutani, T. Akiyama, S. Yamada, K. Takechi, T. Shiga, T. Motohiro, H. Nakayama, K. Kohama, *Jpn. J. Appl. Phys.* 46 (2007) 2632.
- [174] K. Takechi, T. Shiga, T. Akiyama, S. Yamada, *Photochem. Photobiol. Sci.* 9 (2010) 1085.
- [175] A. Brune, G. Jeong, P.A. Liddell, T. Sotomura, T.A. Moore, A.L. Moore, D. Gust, *Langmuir* 20 (2004) 8366.
- [176] T. Akiyama, M. Nakada, N. Terasaki, S. Yamada, *Chem. Commun.* (2006) 395.
- [177] K. Takahashi, M. Asano, K. Imoto, T. Yamaguchi, T. Komura, *J. Phys. Chem. B* 107 (2003) 1646.
- [178] L. Giribabu, C.H.V. Kumar, M. Raghavender, K. Somaiyah, P.Y. Reddy, P.V. Rao, *J. Chem. Sci.* 120 (2008) 455.
- [179] A.F. Nogueira, A.L.B. Formiga, H. Winnischofer, M. Nakamura, F.M. Engelmann, K. Araki, H.E. Toma, *Photochem. Photobiol. Sci.* 3 (2004) 56.
- [180] D. Wróbel, A. Boguta, R.M. Ion, *J. Photochem. Photobiol. A: Chem.* 138 (2001) 7.
- [181] M.G. Harrison, R.H. Friend, in: K. Müllen, G. Wegner (Eds.), *Electronic Materials: The Oligomer Approach*, Wiley-VCH, Weinheim, 1998, p. 515.
- [182] A.J. Mozer, D.L. Officer, *Solar Altern. Energy, SPIE* (2009), doi:10.1117/2.1200911.1701.
- [183] L. Li, S.-W. Kang, J. Harden, Q. Sun, X. Zhou, L. Dai, A. Jakli, S. Kumar, Q. Li, *Liq. Cryst.* 35 (2008) 233.
- [184] K. Takahashi, T. Goda, T. Yamaguchi, T. Komura, *J. Phys. Chem. B* 103 (1999) 4868.
- [185] K. Takahashi, T. Iwanaga, T. Yamaguchi, T. Komura, K. Muratab, *Synth. Met.* 123 (2001) 91.
- [186] F.F. Ajayia, K.-J. Chae, K.-Y. Kima, M.-j. Choia, I.S. Kim, *Int. J. Hydrogen Energy* 34 (2009) 110.
- [187] Y. Tsuchiya, A. Ikeda, T. Konishi, J. Kikuchi, *J. Mater. Chem.* 4 (2004) 1128.
- [188] I. Hanyž, D. Wróbel, *Cryst. Res. Technol.* 38 (2003) 325.
- [189] J. Zhao, B. Li, Z. Bo, *Chin. Sci. Bull.* 51 (2006) 1287.
- [190] R.W. Fessenden, P.V. Kamat, *J. Phys. Chem.* 99 (1995) 12902.
- [191] J. Zimmermann, J. von Gersdorff, H. Kurreck, B. Röder, *J. Photochem. Photobiol. B: Biol.* 40 (1997) 209.
- [192] D. Wróbel, I. Hanyž, R. Bartkowiak, R.M. Ion, *J. Fluorescence* 8 (1988) 191.
- [193] X. He, Y. Zhou, Y. Zhou, L. Wang, T. Li, Z. Bi, M. Zhang, T. Shen, *J. Mater. Chem.* 10 (2000) 873.
- [194] K. Gunaydin, R.-M. Ion, F.I. Scarlat, F. Scarlat, V.I.R. Niculescu, C. Macau, *J. Optoelectron. Adv. Mater.* 6 (2004) 289.
- [195] P.P. Kumar, G. Premaladha, B.G. Maiya, *J. Chem. Sci.* 117 (2005) 193.
- [196] G. Mehta, S. Muthusamy, B.G. Maiya, S. Arounaguir, *J. Chem. Soc. Perkin Trans. 1* (1999) 2177.
- [197] S. Banfi, E. Caruso, M. Gariboldi, S. Alemani, G. Nasini, E. Bombardelli, *Synth. Commun.* 38 (2008) 1096.
- [198] M. Tao, L. Liu, D. Liu, X. Zhou, *Dyes Pigments* 85 (2010) 21.
- [199] H. Imahori, S. Hayashi, H. Hayashi, A. Oguro, S. Eu, T. Umeyama, Y. Matano, *J. Phys. Chem. C* 113 (2009) 18406.
- [200] K. Lewandowska, D. Wróbel, G. Milczarek, *Fullerenes Nanotubes Carbon Nanostruct.* 18 (2010) 262.
- [201] M.C. Martin, X. Du, J. Kwon, L. Mihaly, *Phys. Rev. B* 50 (1994) 173.
- [202] A. Graja, A. Łapiński, S. Król, *J. Mol. Struct.* 404 (1997) 147.
- [203] C. Kang, Z.Y. Lin, *J. Theor. Comput. Chem.* 5 (2006) 665.
- [204] H. Imahori, Y. Sakata, *Adv. Mater.* 9 (1997) 537.
- [205] N. Martin, L. Sánchez, B. Illescas, I. Pérez, *Chem. Rev.* 98 (1998) 2527.
- [206] K. Tamaki, H. Imahori, Y. Nishimura, I. Yamazaki, Y. Sakata, *Chem. Commun.* (1999) 625.
- [207] M.R. Wasielewski, *Chem. Rev.* 92 (1992) 435.
- [208] N. Armaroli, F. Diederich, L. Echegoyen, T. Habicher, L. Flamigni, G. Marconi, J.-F. Nierengarten, *New J. Chem.* (1999) 77.

- [209] F. D'Souza, O. Ito, *Chem. Commun.* (2009) 4913.
- [210] F. D'Souza, S. Gadde, M.E. Zandler, K. Arkady, M.E. El-Khouly, M. Fujitsuka, O. Ito, *J. Phys. Chem. A* 106 (2002) 12393.
- [211] M.E. El-Khouly, Y. Araki, O. Ito, S. Gadde, A.L. McCarty, P.A. Karr, M.E. Zandler, F. D'Souza, *Phys. Chem. Chem. Phys.* 7 (2005) 3163.
- [212] F. D'Souza, G.R. Deviprasad, M.E. Zandler, V.T. Hoang, A. Klykov, M. Van Stipdonk, A. Perera, M.E. El-Khouly, M. Fujitsuka, O. Ito, *J. Phys. Chem. A* 106 (2002) 3243.
- [213] T. Manna, S. Bhattacharya, *J. Theor. Comp. Chem.* 7 (2008) 1055.
- [214] M.A. Herranz, N. Martin, L. Sanchez, C. Seoane, D.M. Guldi, *J. Organometal. Chem.* 599 (2000) 2.
- [215] M.E. El-Khouly, L.M. Rogers, M.E. Zandler, S. Gadde, S.M. Fujitsuka, O. Ito, F.D. Souza, *ChemPhysChem* 4 (2003) 474.
- [216] H. Imahori, M.E. El-Khouly, M. Fujitsuka, O. Ito, Y. Sakata, S. Fukuzumi, *J. Phys. Chem. A* 105 (2001) 325.
- [217] H. Imahori, Y. Sakata, *Eur. J. Org. Chem.* (1999) 2445.
- [218] D. Kuciasukas, P.A. Liddell, S. Lin, S.G. Stone, A.L. Moore, T.A. Moore, D. Gust, *J. Phys. Chem. B* 104 (2000) 4307.
- [219] D.I. Schuster, K. Li, D.M. Guldi, A. Palkar, L. Echegoyen, C. Stanisky, R.J. Cross, M. Niemi, N.V. Tkachenko, H. Lemmetyinen, *J. Am. Chem. Soc.* 129 (2007) 15973.
- [220] J. Ranta, T. Kumpulainen, H. Lemmetyinen, A. Efimov, *J. Org. Chem.* 75 (2010) 5178.
- [221] V. Vehmanen, N.V. Tkachenko, A. Efimov, P. Damlin, A. Ivaska, H. Lemmetyinen, *J. Phys. Chem.* 106 (2002) 8029.
- [222] A. Graja, A. Łapiński, B. Laskowska, I. Olejniczak, A. Bogucki, *Mol. Cryst. Liq. Cryst.* 483 (2008) 1.
- [223] A. Graja, I. Olejniczak, A. Bogucki, D. Bonifazi, F. Diederich, *Chem. Phys.* 300 (2004) 227.
- [224] A. Łapiński, A. Graja, I. Olejniczak, A. Bogucki, H. Imahori, *Chem. Phys.* 305 (2004) 277.
- [225] A. Graja, D. Wróbel, A. Boguta, I. Olejniczak, A. Bogucki, *Synth. Met.* 152 (2005) 97.
- [226] A. Łapiński, A. Graja, I. Olejniczak, A. Bogucki, *J. Mol. Struct.* 792–793 (2006) 2.
- [227] D. Wróbel, A. Graja, H. Manikowski, K. Lewandowska, *Chem. Phys.* 336 (2007) 165.
- [228] M.J. Frisch, G.W. Trucks, H.B. Schlegel, G.E. Scuseria, M.A. Robb, J.R. Cheeseman, J.A. Montgomery Jr., T. Vreven, K.N. Kudin, J.C. Burant, J.M. Millam, S.S. Iyengar, J. Tomasi, V. Barone, B. Mennucci, M. Cossi, G. Scalmani, N. Rega, G.A. Petersson, H. Nakatsuji, M. Hada, M. Ehara, K. Toyota, R. Fukuda, J. Hasegawa, M. Ishida, T. Nakajima, Y. Honda, O. Kitao, H. Nakai, M. Klene, X. Li, J.E. Knox, H.P. Hratchian, J.B. Cross, C. Adamo, J. Jaramillo, R. Gomperts, R.E. Stratmann, O. Yazyev, A.J. Austin, R. Cammi, C. Pomelli, J.W. Ochterski, P.Y. Ayala, K. Morokuma, G.A. Voth, P. Salvador, J.J. Dannenberg, V.G. Zakrzewski, S. Dapprich, A.D. Daniels, M.C. Strain, O. Farkas, D.K. Malick, A.D. Rabuck, K. Raghavachari, J.B. Foresman, J.V. Ortiz, Q. Cui, A.G. Baboul, S. Clifford, J. Cioslowski, B.B. Stefanov, G. Liu, A. Liashenko, P. Piskorz, I. Komaromi, R.L. Martin, D.J. Fox, T. Keith, M.A. Al-Laham, C.Y. Peng, A. Nanayakkara, M. Challacombe, P.M.W. Gill, B. Johnson, W. Chen, M.W. Wong, C. Gonzalez, J.A. Pople, *Gaussian 03*, Revision D.01, Wallingford CT, 2004.
- [229] K. Itoh, K. Nakahashi, H. Toeda, *J. Phys. Chem.* 92 (1988) 1464.
- [230] L.L. Gladkov, N.M. Ksenofontova, K.N. Soloviev, A.S. Starukhin, A.M. Shulga, A.T. Gradiushko, *Zh. Prikl. Spectr.* 38 (1983) 598.
- [231] X.-Y. Li, M.Z. Zgierski, *J. Phys. Chem.* 95 (1991) 4268.
- [232] R.E. Stanton, M.D. Newton, *J. Phys. Chem.* 92 (1988) 2141.
- [233] I. Olejniczak, A. Graja, A. Bogucki, M. Golub, P. Hudhomme, A. Gorgues, D. Kreher, M. Cariou, *Synth. Met.* 126 (2002) 263.
- [234] M.A. Tanatar, A. Graja, D.B. Zhu, Y.L. Li, *Synth. Met.* 94 (1998) 83.
- [235] H. Manikowski, D. Wróbel, K. Lewandowska, A. Graja, *Synth. Met.* 157 (2007) 363.
- [236] F. D'Souza, R. Chitta, K. Ohkubo, M. Tasior, N.K. Subbaiyan, M.E. Zandler, M.K. Rogacki, D.T. Gryko, S. Fukuzumi, *J. Am. Chem. Soc.* 130 (2008) 14263.
- [237] A.W. Johnson, I.T. Kay, *J. Chem. Soc.* (1965) 1620.
- [238] Z. Gross, N. Galili, I. Saltsman, *Angew. Chem. Int. Ed.* 38 (1999) 1427.
- [239] D.T. Gryko, *Eur. J. Org. Chem.* (2002) 1735.
- [240] B. Ventura, A. Degli Esposti, B. Koszerna, D.T. Gryko, L. Flamigni, *New J. Chem.* 29 (2005) 1559.
- [241] J. Poulin, C. Stern, R. Guillard, D. Harvey, *Photochem. Photobiol.* 82 (2006) 171.
- [242] F. D'Souza, E. Maligaspe, P.A. Karr, A.L. Schumacher, M.L. Oijami, C.P. Gros, J.-M. Barbe, K. Ohkubo, S. Fukuzumi, *Chem. Eur. J.* 14 (2008) 674.
- [243] L. Flamigni, B. Ventura, M. Tasior, T. Becherer, H. Langhals, D.T. Gryko, *Chem. Eur. J.* 14 (2008) 169.
- [244] P.J. Brache, D.I. Schuster, in: D.M. Guldi, N. Martin (Eds.), *Fullerenes: From Synthesis to Optoelectronic Properties*, Kluwer Academic Publishers, Dordrecht, 2002, p. 163 (Chapter 6).
- [245] G. Kodja, P.A. Liddell, L. Garza, P.C. Clausem, J.S. Lindley, A.L. Moore, T.A. Moore, D. Gust, *J. Phys. Chem. A* 106 (2002) 2036.
- [246] K. Yamada, H. Imahori, Y. Nishimura, I. Yamazaki, Y. Sakata, *Chem. Lett.* 9 (1999) 895.
- [247] B. Jiang, S. Yang, S. Jones Jr., *Chem. Mater.* 9 (1997) 2031.
- [248] S.A. Vail, J.P.C. Tomé, P.J. Krawczuk, A. Dourandin, V. Shafirovich, J.A.S. Cavaleiro, D.I. Schuster, *J. Phys. Org. Chem.* 17 (2004) 814.
- [249] B. Barszcz, B. Laskowska, A. Graja, E.Y. Park, T.-D. Kim, K.-S. Lee, *Synth. Met.* 161 (2011) 229.
- [250] B. Barszcz, B. Laskowska, A. Graja, E.Y. Park, T.-D. Kim, K.-S. Lee, *Chem. Phys. Lett.* 479 (2009) 224.
- [251] R. Gómez, J.L. Segura, N. Martín, *Org. Lett.* 7 (2005) 717.
- [252] J. Baffreau, L. Perrin, S. Leroy-Lhez, P. Hudhomme, *Tetrahedron Lett.* 46 (2005) 4599.
- [253] H. Imahori, K. Yamada, M. Hasegawa, S. Taniguchi, T. Okada, Y. Sakata, *Angew. Chem. Int. Ed. Eng.* 36 (1997) 2626.
- [254] D. Kuciasukas, P.A. Liddell, A.L. Moore, T.A. Moore, D. Gust, *J. Am. Chem. Soc.* 120 (1998) 10880.
- [255] H. Imahori, D.M. Guldi, K. Tamaki, Y. Yoshida, C. Luo, Y. Sakata, S. Fukuzumi, *J. Am. Chem. Soc.* 123 (2001) 6617.
- [256] M. Fujitsuka, O. Ito, H. Imahori, K. Yamada, H. Yamada, Y. Sakata, *Chem. Lett.* (1999) 721.
- [257] H. Imahori, *J. Phys. Chem. B* 108 (2004) 6130.
- [258] J.S. Lindsey, *New J. Chem.* 15 (1991) 153.
- [259] D. Philip, J.F. Stoddart, *Angew. Chem. Int. Ed.* 35 (1996) 1154.
- [260] T. Akiyama, H. Imahori, A. Ajavakom, Y. Sakata, *Chem. Lett.* (1996) 907.
- [261] H. Imahori, H. Yamada, S. Ozawa, K. Ushida, Y. Sakata, *Chem. Commun.* (1999) 1165.
- [262] R.B. Bazaco, J.L. Segura, C. Seoane, *Collect. Czech. Chem. Commun.* 74 (2009) 857.
- [263] H.-Y. Zhao, C. Chen, Y.-Z. Zhu, J.-Y. Zheng, *Chem. J. Chin. Univ.* 31 (2010) 933.
- [264] M.E. El-Khouly, D.K. Ju, K.-Y. Kay, F. D'Souza, S. Fukuzumi, *Chem.: A Eur. J.* 16 (2010) 6193.
- [265] E. Maligaspe, N.V. Tkachenko, N.K. Subbaiyan, R. Chitta, M.E. Zandler, H. Lemmetyinen, F. D'Souza, *J. Phys. Chem. A* 113 (2009) 8478.
- [266] F. D'Souza, S. Gadde, A.L. Shumacher, M.E. Zandler, A.S.D. Sandanayaka, Y. Araki, O. Ito, *J. Phys. Chem. C* 111 (2007) 11123.
- [267] T. Nakamura, J.-Y. Ikemoto, M. Fujitsuka, Y. Araki, O. Ito, K. Takimiya, Y. Aso, T. Otsubo, *J. Phys. Chem. B* 109 (2005) 14365.
- [268] D. Blaudet, T. Buffeteau, B. Desbat, P. Fournier, A.-M. Ritcey, M. Pézolet, *J. Phys. Chem. B* 102 (1998) 99.
- [269] T. Samurai, R. Fukasawa, S. Kawai, K. Akimoto, *Jpn. J. Appl. Phys.* 45 (2006) 397.
- [270] R. Naito, S. Toyoshima, T. Ohashi, T. Sakurai, K. Akimoto, *Jpn. J. Appl. Phys.* 47 (2008) 1416.
- [271] I. Fratoddi, C. Battocchio, R. D'Amato, G.P. Di Egidio, L. Ugo, G. Polzonetti, M.V. Russo, *Mater. Sci. Eng. C* 23 (2003) 867.
- [272] K. Lewandowska, A. Bogucki, D. Wróbel, A. Graja, *J. Photochem. Photobiol. A: Chem.* 188 (2007) 12.
- [273] G.J. Simpson, K.L. Rowien, *Acc. Chem. Res.* 33 (2000) 781.
- [274] R.G. Greenler, *J. Phys. Chem.* 44 (1966) 310.
- [275] D.L. Allara, J.D. Swalen, *J. Phys. Chem.* 88 (1982) 574.
- [276] M.K. Debe, *J. Appl. Phys.* 55 (1984) 3354.
- [277] R. Arnold, A. Terfort, Ch. Wöll, *Langmuir* 17 (2001) 4980.
- [278] W.G. Golden, in: J.R. Ferraro, L.J. Basile (Eds.), *Fourier Transform Infrared Spectroscopy*, Academic Press, Orlando, 1985, p. 315.
- [279] K. Lewandowska, D. Wróbel, A. Biadasz, R. Świetlik, *J. Photochem. Photobiol. A: Chem.* 200 (2008) 225.
- [280] A. Graja, K. Lewandowska, B. Laskowska, A. Łapiński, D. Wróbel, *Chem. Phys.* 352 (2008) 339.
- [281] K. Lewandowska, A. Graja, B. Barszcz, A. Biadasz, D. Wróbel, *New J. Chem.* (2010), doi:10.1039/c0nj00766h.
- [282] A. Biadasz, B. Bursa, B. Barszcz, A. Bogucki, D. Wróbel, A. Graja, *Dyes Pigments* 89 (2011) 86, doi:10.1016/j.dyepig.2010.09.008.
- [283] H. Arwin, D.E. Aspnes, *Thin Solid Films* 138 (1986) 195.
- [284] Y.-T. Kim, D.L. Allara, R.W. Collins, K. Vedam, *Thin Solid Films* 193 (1990) 350.
- [285] D.L. Allara, R.G. Nuzzo, *Langmuir* 1 (1985) 52.
- [286] S.B. Dierker, C.A. Murray, J.D. Langrange, N.E. Schlotter, *Chem. Phys. Lett.* 137 (1987) 453.
- [287] S.R. Wasserman, G.M. Whitesides, I.M. Tidswell, B.M. Ocko, P.S. Pershan, J.D. Axe, *J. Am. Chem. Soc.* 111 (1989) 5852.
- [288] S.H. Chen, C.W. Frank, *Langmuir* 5 (1989) 978.
- [289] M. Yoneyama, M. Sugi, M. Saito, K. Ikegami, S. Kuroda, S. Iizima, *Jpn. J. Appl. Phys.* 25 (1986) 961.
- [290] J.R. Durrant, S.A. Haque, E. Palomares, *Coord. Chem. Rev.* 248 (2004) 1247.
- [291] D.M. Guldi, *Phys. Chem. Chem. Phys.* 9 (2007) 1400.
- [292] D. Wöhrle, D. Meissner, *Adv. Mater.* 3 (1991) 129.
- [293] T.L. Benanti, D. Venkataraman, *Photosynth. Res.* 87 (2006) 73.
- [294] H. Hoppe, N.S. Sariciftci, *J. Mater. Res.* 19 (2004) 1924.
- [295] M. Grätzel, *J. Photochem. Photobiol. A: Chem.* 164 (2004) 3.
- [296] C.D. Dimitrakopoulos, D.J. Mascaro, *IBM J. Res. Dev.* 45 (2001) 11.
- [297] J.M. Halls, K. Pichler, R.H. Friend, S.C. Moratti, A.B. Holmes, *Appl. Phys. Lett.* 68 (1996) 3120.
- [298] H.R. Kerp, H. Donker, R.B.M. Koehorst, T.J. Schaafsma, E.E. van Fassen, *Chem. Phys. Lett.* 298 (1998) 302.
- [299] P. Peumans, A. Yakimov, S.R. Forrest, *J. Appl. Phys.* 93 (2003) 3693.
- [300] C.W. Tang, *Appl. Phys. Lett.* 48 (1986) 183.
- [301] J. Rostalski, D. Meissner, *Sol. Energy Mater. Sol. Cells* 61 (2000) 1.
- [302] D. Gebeyehu, B. Maening, J. Drechsel, K. Leo, M. Pfeiffer, *Sol. Energy Mater. Sol. Cells* 79 (2003) 81.
- [303] M. Hiramoto, H. Fujiwara, M. Yokoyama, *J. Appl. Phys.* 72 (1992) 3781–3787.
- [304] J. Xue, S. Uchida, B.P. Rand, S.R. Forrest, *Appl. Phys. Lett.* 84 (2004) 3013.
- [305] M. Hiramoto, M. Suezaki, M. Yokoyama, *Chem. Lett.* (1990) 327.
- [306] *Organic Photovoltaics*, *Acc. Chem. Res.* 42 (special issue) (2009).